Sulfur-bearing phases detected by evolved gas analysis of the Rocknest aeolian deposit, Gale Crater, Mars

Authors:
Amy C. McAdam[1*], Heather B. Franz[1,2], Brad Sutter[3,4], Paul D. Archer, Jr.[3,4], Caroline Freissinet[1], Jennifer L. Eigenbrode[1], Douglas W. Ming[4], Sushil K. Atreya[5], David L. Bish[6], David F. Blake[7], Hannah E. Bower[1], Anna Brunner[1,8], Arnaud Buch[9], Daniel P. Glavin[1], John P. Grotzinger[10], Paul R. Mahaffy[1], Scott M. McLennan[11], Richard V. Morris[4], Rafael Navarro-González[12], Elizabeth B. Rampe[4], Steven W. Squyres[13], Andrew Steele[14], Jennifer C. Stern[1], Dawn Y. Sumner[15], James J. Wray[16]

Affiliations:
[1]NASA Goddard Space Flight Center, Greenbelt, Maryland, USA
[2]Center for Research and Exploration in Space Science & Technology, Department of Astronomy, University of Maryland Baltimore County, Baltimore, Maryland, USA
[3]Jacobs, Houston, Texas, USA
[4]Astromaterials Research and Exploration Science Directorate, NASA Johnson Space Center, Houston, Texas, USA
[5]Department of Atmospheric, Oceanic and Space Sciences, University of Michigan, Ann Arbor, Michigan, USA
[6]Department of Geological Sciences, Indiana University, Bloomington, Indiana, USA
[7]NASA Ames Research Center, Moffett Field, California, USA
[8]Center for Research and Exploration in Space Science & Technology, Department of Astronomy, University of Maryland College Park, College Park, Maryland, USA
[9]LGPM, Ecole Centrale Paris, Chatenay-Malabry, France
[10]Division of Geological and Planetary Sciences, California Institute of Technology, Pasadena, California, USA
[11]Department of Geosciences, Stony Brook University, Stony Brook, New York, USA
[12]Laboratorio de Química de plasmas y Estudios Planetarios, Instituto de Ciencias Nucleares, Universidad Nacional Autónoma de México, Ciudad Universitaria, México D.F., Mexico
[13]Department of Astronomy, Cornell University, Ithaca, New York, USA
[14]Geophysical Laboratory, Carnegie Institution of Washington, Washington DC, USA
[15]Department of Earth and Planetary Sciences, University of California, Davis, California, USA
[16]School of Earth and Atmospheric Sciences, Georgia Institute of Technology, Atlanta, Georgia, USA
*Corresponding author: A. C. McAdam, NASA Goddard Space Flight Center, 8800 Greenbelt Road, Code 699, Greenbelt, Maryland, 20771, USA. (Amy.McAdam@nasa.gov)

This article has been accepted for publication and undergone full peer review but has not been through the copyediting, typesetting, pagination and proofreading process which may lead to differences between this version and the Version of Record. Please cite this article as doi: 10.1002/2013JE004518

Abstract

The Sample Analysis at Mars (SAM) instrument suite detected SO_2, H_2S, OCS and CS_2 from ~450-800 ºC during evolved gas analysis (EGA) of materials from the Rocknest aeolian deposit in Gale Crater, Mars. This was the first detection of evolved sulfur species from a martian surface sample during *in situ* EGA. SO_2 (~3-23 μmol) is consistent with the thermal decomposition of Fe-sulfates or Ca-sulfites, or evolution/desorption from sulfur-bearing amorphous phases. Reactions between reduced sulfur phases such as sulfides and evolved O_2 or H_2O in the SAM oven are another candidate SO_2 source. H_2S (~41-109 nmol) is consistent with interactions of H_2O, H_2 and/or HCl with reduced sulfur phases and/or SO_2 in the SAM oven. OCS (~1-5 nmol) and CS_2 (~0.2-1 nmol) are likely derived from reactions between carbon-bearing compounds and reduced sulfur. Sulfates and sulfites indicate some aqueous interactions, although not necessarily at the Rocknest site; Fe-sulfates imply interaction with acid solutions whereas Ca-sulfites can form from acidic to near-neutral solutions. Sulfides in the Rocknest materials suggest input from materials originally deposited in a reducing environment, or from detrital sulfides from an igneous source. The presence of sulfides also suggests that the materials have not been extensively altered by oxidative aqueous weathering. The possibility of both reduced and oxidized sulfur compounds in the deposit indicates a non-equilibrium assemblage. Understanding the sulfur mineralogy in Rocknest materials, which exhibit chemical similarities to basaltic fines analyzed elsewhere on Mars, can provide insight in to the origin and alteration history of martian surface materials.

1. Introduction

The first sampling location for the Mars Science Laboratory (MSL) *Curiosity* rover on Mars was at an aeolian deposit informally named Rocknest. Rocknest is described in detail elsewhere [*Blake et al.*, 2013] and was selected primarily because of its loose, granular nature which was required to clean the *Curiosity's* sample acquisition, handling and processing system, as well as providing important new measurements on windblown materials on Mars. Rocknest is a small aeolian deposit (sand shadow) 15 cm high and 7 meters long that formed in the wind shadow produced by a group of rocks (Figure 1). It is armored with particles 1-3 mm in diameter and is covered with bright airfall dust deposits suggesting that it is not presently active [*Blake et al.*, 2013]. Its interior is composed primarily of darker, <150 μm size particles.

Rocknest materials are geochemically important because they contain a component of martian surface fines. Widely spread, previous surface *in situ* investigations of martian surface fines [e.g., *Bruckner et al.*, 2003; *Clark et al.*, 1982; *Gellert et al.*, 2006] have indicated that their overall sulfur chemistry and bulk chemistry exhibit only minor variation even over global scales. The Rocknest deposit is chemically very similar to surface materials analyzed at several other locations on Mars suggesting homogenization of near surface basaltic crustal materials that are largely similar across the surface of Mars by a combination of impact and aeolian processes [*Gellert et al.*, 2006; *Yen et al.*, 2013; *Yen et al.*, 2005]. The mineralogy and provenance of Rocknest materials may therefore be relevant for understanding global-scale distribution of materials and the composition of local rocks.

Sulfur-bearing phases provide important insight into possible martian surface processes and past or present habitability. The presence of oxidized sulfur phases, such as sulfates, suggests that aqueous alteration played a role in their formation

either within the material or prior to their incorporation in the materials [e.g., *Bibring et al.*, 2006; *Squyres and Knoll*, 2005; *Tosca et al.*, 2004]. The presence of reduced sulfur phases, such as sulfides, might indicate a contribution from materials deposited in a reducing environment, or indicate that the material incorporated detrital igneous pyrite or pyrrhotite and remained a relatively dry setting such that the sulfide has not subsequently been oxidized [e.g., *Burns and Fisher*, 1990; *Jambor et al.*, 2000; *Zolotov and Shock*, 2005].

The objectives of this paper are to describe the volatile sulfur-bearing species evolved from Rocknest materials and constrain the possible S-bearing phases that evolved those volatile species. The Sample Analysis at Mars (SAM) instrument was used to characterize the volatile sulfur content of Rocknest. SAM consists of a quadrupole mass spectrometer (QMS), a 6-column gas chromatograph (GC), and a tunable laser spectrometer (TLS) that are interfaced with gas and solid sample processing systems, including sample pyrolysis ovens [*Leshin et al.*, 2013; *Mahaffy et al.*, 2012]. These instruments analyze gases evolved by pyrolysis of samples, as well as atmospheric gases.

2. Sulfur and sulfur compounds on the martian surface

Gamma-ray spectral mapping of the martian surface indicates an elevated regional-scale sulfur content of about 2 wt% on average to at least several decimeter depths [*King and McLennan*, 2010; *McLennan et al.*, 2010]. Viking thermal analysis to 500 ^{o}C by the molecular analysis experiment did not detect S-bearing volatiles [*Biemann et al.*, 1976], though the lander did investigate the surprisingly S- (and Cl-) rich surface materials *in situ* for the first time e.g., [*Clark et al.*, 1976]. Surface soils at all landing sites visited since have also exhibited this S- and Cl-rich character that is thought to be largely related to a large scale or perhaps even global component.

The Pathfinder rover also detected bulk sulfur compositions similar to Viking surface materials [e.g., *Rieder et al.*, 1997], but did not have a thermal analysis capability or any other analytical tool capable of evaluating the volatile content of surface materials at the landing site.

Sulfates have been directly detected or strongly inferred from geochemical relationships at both MER landing sites. At Meridiani Planum, the sedimentary bedrock is a "dirty evaporite" consisting of roughly 20% Mg-sulfates, 10% Fe-sulfate, and 10% Ca-sulfate [*Squyres and Knoll*, 2005]. The waters from which the evaporation took place were probably low-pH brines, based on evidence for Fe-sulfate phases such as jarosite [*Dyar et al.*, accepted; *Klingelhofer et al.*, 2004; *Morris et al.*, 2006]. The concentration of Mg-sulfate, the most water-soluble sulfate present, varies with depth, suggesting that water interacted with the sediments after their deposition. Centimeter-thick veins of nearly pure Ca-sulfate, probably gypsum, have also been found near the rim of Endeavour Crater [*Squyres et al.*, 2012].

Sulfates were also found in the Columbia Hills at Gusev Crater. The most noteworthy sulfate-rich bedrock outcrops in the Columbia Hills are the Peace class rocks [*Ming et al.*, 2006], which are ultramafic sandstones cemented by 15-20% Mg- and Ca-sulfates. Trenches dug with the rover wheels in the soils of the Gusev Crater plains contain high and vertically variable concentrations of Mg-sulfates [*Wang et al.*, 2006], suggesting mobilization by migrating fluids. The highest concentrations of sulfates at Gusev are found in the highly localized Paso Robles class soils [*Yen et al.*, 2008]. Paso Robles soils are dominated by ferric iron sulfates (e.g., ferricopiapite), silica, and Mg-sulfates; Ca-sulfates are also present in some samples [*Lane et al.*, 2008; *Ming et al.*, 2006; *Wang et al.*, 2006; *Wang and Ling*, 2011]. The chemical compositions of these soils clearly reflect the elemental signatures of nearby rocks

(Wishstone and Watchtower class rocks), and they likely formed as hydrothermal and fumarolic condensates [*Ming et al.*, 2006; *Yen et al.*, 2008].

The Phoenix lander found evidence for minor sulfates in polar martian soils, but this evidence was from the Wet Chemistry Laboratory (WCL) experiment that measured ions in solution; evolved sulfur species were not detected during Phoenix Thermal and Evolved Gas Analyzer (TEGA) analyses [*Kounaves et al.*, 2010]. WCL analyses, together with geochemical modeling, were used to infer the presence of ~3.3 wt% Mg- and Ca-sulfate [*Kounaves et al.*, 2010] in the polar materials. These sulfates could have been sourced by windblown input from the gypsum-rich dune fields to the north [e.g., *Langevin et al.*, 2005], implying formation by previous water-rock interactions before being wind transported to the Phoenix site. They could have also resulted from interactions between H_2SO_4-bearing aerosols (for example formed by atmospheric oxidation of volcanic SO_2 and H_2S) and soil constituents [e.g., *Kounaves et al.*, 2010]. Although TEGA did not detect evolved sulfur species that would have supported the presence of the sulfur-bearing phases, the temperatures reached by TEGA (~1000 ^{o}C) [*Hoffman et al.*, 2008] may have been insufficient to cause thermal breakdown of Ca-sulfate phases under TEGA operating conditions [*Golden et al.*, 2009].

Sulfates have been observed or inferred via orbital spectroscopy in a wide range of regions on Mars. Near-infrared reflectance spectroscopy first measured gypsum ($CaSO_4 \bullet 2H_2O$) in sand dunes surrounding the north polar cap [*Langevin et al.*, 2005] and both monohydrated and polyhydrated sulfates in equatorial layered deposits within Valles Marineris, Meridiani Planum, and the chaos terrains in between them [*Gendrin et al.*, 2005]. Such layered sulfates have now been identified in other middle latitude sites as well [*Wray et al.*, 2009], and in Gale Crater's Mt. Sharp

[*Milliken et al.*, 2010]. The mono- and polyhydrated sulfates are commonly interpreted as Mg-rich but could alternatively be Fe^{2+} or Fe^{3+}-bearing sulfates in many cases [*Bishop et al.*, 2009; *Wiseman et al.*, 2010; *Wray et al.*, 2011]. In a few scattered, localized outcrops, sulfates that form under acidic conditions, such as jarosite and/or alunite, have been found [e.g., *Farrand et al.*, 2009; *Milliken et al.*, 2008; *Wray et al.*, 2011]. Deposits enriched in Ca-sulfates have also been found outside the polar regions [*Mangold et al.*, 2010; *Wray et al.*, 2010], demonstrating a diversity of sulfate chemistries recorded in the martian rock record. Modeling of orbital thermal infrared spectra has allowed estimation of sulfate abundances (16 vol %) in at least one layered sulfate outcrop in Columbus Crater [*Baldridge et al.*, 2013].

The above infrared measurements are not sensitive to the sulfur-bearing phases inferred in global soils by the landed missions, possibly because of detection limits or the difficulty in identifying certain sulfur phases (e.g., amorphous S-bearing phases) in these "spectrally bland" soils. The Mars Odyssey Gamma Ray Spectrometer (GRS) is sensitive to average soil sulfur, however. Although Ca- and Mg-sulfates seem the likeliest sulfates in indurated soils in specific regions [*Karunatillake et al.*, 2009], the GRS-measured H:S stoichiometry suggests Fe-bearing sulfates as a key hydration phase in most areas, along with chemically complex mixtures of variably hydrated sulfates [*Karunatillake et al.*, 2012]. In particular, even in the southern hemisphere where H and S associate most strongly, up to 50% of the sulfur by mass may exist in anhydrous phases.

The high concentrations of sulfur in the martian surface environment (2 wt% on average to several decimeter depths [*King and McLennan*, 2010; *McLennan et al.*, 2010]), coupled with the occurrence of a variety of Fe^{3+}-sulfate phases, and detection of only minor amounts of carbonate minerals has led to the suggestion that some form

of an sulfur-cycle has dominated surficial processes over much of martian geological history [e.g., *Gaillard et al.*, 2013; *Halevy et al.*, 2007; *Johnson et al.*, 2008; *King and McLennan*, 2010; *King and McSween*, 2005; *McLennan*, 2012; *McLennan and Grotzinger*, 2008]. A dominant S cycle would make low-pH aqueous conditions quite likely. There are several scenarios that have been suggested to provide the acidic conditions that could result in the relatively high sulfur surface materials observed. These include alteration of rocks and sediment by acid aerosols [*Banin et al.*, 1997; *Settle*, 1979; *Tosca et al.*, 2004], low temperature alteration [e.g., *Bridges et al.*, 2001; *Clark and Vanhart*, 1981; *Hurowitz et al.*, 2006; *McSween and Keil*, 2000; *Morris et al.*, 2000; *Niles and Michalski*, 2009], some hydrothermal settings associated with impacts or volcanic activity [e.g., *Baker et al.*, 2000; *Newsom et al.*, 1999], or acid lake systems [*Benison and Laclair*, 2003]. In addition, because ferric iron is far more soluble when under low-pH conditions, there is likely to be a strong linkage between the iron/oxygen cycles and the S-cycle [e.g., *Bibring et al.*, 2007; *Bibring et al.*, 2006; *McLennan*, 2012; *Tosca et al.*, 2008]. Accordingly, working to understand the relationships between iron and sulfur mineralogy in martian surficial deposits should help constrain such scenarios. Secondary sulfur phases in Rocknest materials, which show similarities to martian surface fines analyzed at several locations on Mars and likely contain Fe-sulfates, are likely to have at least partially formed from these types of processes.

As detailed above, there is abundant evidence for a significant, widespread sulfur-bearing component or components in martian surface materials. In the majority of cases, these sulfur-bearing components in materials exposed to the relatively oxidizing martian surface environment were either inferred or observed to be sulfates. Although there are regions on Mars (e.g., the Opportunity landing site) that have

sulfur-rich bedrock and the physical weathering of these sorts of rocks can contribute sulfur to martian soils and windblown materials, the consistent signature of S-rich materials across the surface may imply a contribution from a widespread process (e.g., alteration by acid aerosols [*Banin et al.*, 1997; *Settle*, 1979; *Tosca et al.*, 2004]) as well. Because the Rocknest deposit sampled by MSL contains aeolian materials, it is reasonable to anticipate an oxidized sulfur component.

Rocknest materials can also be expected to be dominated by primary igneous materials derived from basalt, which can include primary reduced sulfur phases, e.g., pyrite or pyrrhotite. Martian meteorites, which are igneous rocks that in some cases show minor degrees of aqueous alteration, contain small amounts of oxidized sulfur phases and small amount of reduced sulfur phases [e.g., *Gooding*, 1992; *Greenwood et al.*, 1997; *McCubbin et al.*, 2009; *Steele et al.*, 2013]. Orbital and *in situ* investigations have not previously found evidence for reduced S phases, except for a tentative detection of pyrite (FeS_2) at Home Plate by the Mars Exploration Rover (MER) Spirit using Mössbauer spectroscopy [*Morris et al.*, 2008]. Below we discuss evidence from SAM analyses for both reduced and oxidized sulfur phases in the Rocknest materials.

3. Methods

3.1. SAM analyses of Rocknest fines

The QMS, TLS and GC components of SAM are connected to each other by a gas processing system which includes sample pyrolysis ovens. The TLS can provide isotopic analyses and abundances of CO_2, H_2O and CH_4 in gases evolved on heating a sample (or in atmospheric gases). The six-column GC can provide analyses of organic and also inorganic gases evolved during sample pyrolysis. Direct analysis of evolved sample gases by the QMS, a technique referred to as evolved gas analysis

mass spectrometry (EGA will be used hereafter), monitors volatiles evolved as a sample is heated resulting in signal vs. temperature curves referred to as EGA traces. Further details of SAM instrument components and operation can be found in *Mahaffy et al.* [2012] and *Leshin et al.* [2013].

Although we also discuss supporting data from SAM GCMS analyses, the primary focus of this paper is on SAM EGA data from Rocknest samples. To investigate constraints on the phases responsible for the sulfur species evolved during the SAM EGA analysis, EGA of candidate phases in SAM-like laboratory systems was carried out (details of laboratory analyses below). Overall, the combination of which gases are evolved from a sample on heating as a result of mineral thermal decomposition (e.g., dehydration of hydrated minerals, decarbonation of carbonates, etc.) and the temperature at which each gas is evolved can provide constraints on mineralogy [e.g., *Charsley et al.*, 1987; *Milodowski and Morgan*, 1980; *Morgan et al.*, 1988]. However, several factors can affect EGA data such as sample grain size or reactions between sample species, especially in complex samples such as the Rocknest materials, and these factors must be carefully considered, as discussed below [*Bish and Duffy*, 1990]. As a result, EGA is not a definitive mineralogical technique. Although the abundances of evolved gases from a sample can be quantified, EGA traces from complex unknown samples cannot necessarily be quantitatively deconvolved to infer sample volatile-bearing mineral abundances through comparison to EGA data from single minerals and simple mineral mixtures. Nevertheless, comparisons of EGA gas evolution traces from these materials with EGA gas evolution data from complex unknown samples such as the Rocknest samples can provide key constraints on mineralogy, especially in the context of other types of chemical and mineralogical analyses such as X-ray diffraction (XRD) and

Alpha Particle X-ray Spectrometer (APXS) analyses. This approach can support the identification of volatile-bearing minerals identified with other techniques and, importantly, it can provide key evidence for volatile-bearing phases that are present below the detection limit of other techniques or are difficult to characterize with other techniques [e.g., *Charsley et al.*, 1987; *Milodowski and Morgan*, 1980; *Morgan et al.*, 1988].

Curiosity's Collection and Handling for Interior Martian Rock Analysis (CHIMRA) system collected five scoop samples from the Rocknest deposit but only delivered material from the 5th scoop that had been sieved to less than 150 μm. Four portions (< 76 mm^3 each) were delivered into four of SAM's quartz glass sample cups (which had been previously cleaned by heating to >800 ^{o}C) via the SAM Solid Sample Inlet Tube (SSIT) [*Leshin et al.*, 2013]. Four portions of this material were analyzed because several runs were required to carry out needed analyses with GC and TLS. EGA data are acquired during all SAM analyses over the entire heating ramp, but if a GC or TLS analysis is desired, a portion of gas evolved over a given temperature range (referred to as a "cut") can be sent to either the GC or the TLS but not both at the same time. Four runs were needed to obtain GC and TLS cuts to address a variety of science questions. Because these science drivers were not specifically related to evolved sulfur phases they will not be discussed in detail here but they are detailed in *Leshin et al.* [2013]. The four separate portions delivered to SAM are designated here as Rocknest 1, Rocknest 2, Rocknest 3 and Rocknest 4. After sample delivery, the sample cup was sealed inside a pyrolysis oven. The mass of the delivered portions could not be measured directly, but based on tests with MSL testbed hardware the delivered sample mass was estimated to be 50 ± 8 mg (2σ standard deviations) [*Anderson et al.*, 2012; *Leshin et al.*, 2013].

Delivered samples were heated from ~30 ºC (ambient temperature in SAM) to ~835 ºC at a temperature ramp rate of 35 ºC/min with a flow of ~0.8 standard cubic centimeters per minute (sccm) of He over the sample under a pressure of ~30 mbar. A small fraction of the evolved gases was monitored directly with the QMS through a gas split (~1 part in 800 sent to the QMS); this constitutes SAM's EGA mode.

Gases from a selected temperature range during pyrolysis were sent to the GCMS hydrocarbon trap set at an initial temperature of 5 ºC. The hydrocarbon trap was then heated to ~300 ºC to release the trapped volatiles under He flow and transfer them to the GC system for separation and detection by a thermal conductivity detector (TCD) and a QMS. The chromatographic column used for separation was GC5 (MXT-CLP, 30 m x 0.25 mm x 0.25 μm). The GCMS mode can enable better separation of evolved organic compounds but can also allow more definitive identification of inorganic volatiles.

Abundances of evolved SO_2 were based on analysis of SO_2 evolved during pyrolysis of a known mass of a sulfate calibration sample ($FeSO_4 \cdot 4H_2O$) in SAM before launch. There are no pre-launch SAM data for H_2S, OCS, and CS_2, so literature values for the ionization cross sections of these molecules were used in those abundance calculations [*Vinodkumar et al.*, 2010]. The steps involved in these abundance calculations are detailed in the companion paper by *Archer et al.* [2013a].

3.2. Analyses of Rocknest-relevant analogs with SAM-like laboratory systems

Three laboratory systems were used to characterize relevant analog samples for comparison with the SAM Rocknest results. The SAM breadboard consists of a pyrolysis oven and QMS that were custom built to closely mimic the conditions of SAM [*Franz et al.*, 2011; *Mahaffy et al.*, 2012]. Two other EGA laboratory systems (a Hiden EGA-MS system and an Agilent EGA-MS system) are of lower fidelity but

were programmed to operate under conditions as close to SAM conditions as possible. The Hiden EGA-MS system consists of a Hiden HPR-20 QMS coupled to a gas manifold and custom-built sample oven. Powdered samples are heated at 20 ^{o}C/min from ~50 ºC to ~1000-1110 ºC, under SAM-like helium pressures (~30 mb) and gas flow conditions (~1 sccm). The 20 ºC/min heating rate was used in the Hiden EGA-MS system in order to compensate for the slower scan speed of this mass spectrometer compared with the other laboratory systems; this ramp rate enabled a time sampling comparable to other systems while still producing EGA profiles comparable to those from analysis of standards on the other systems. The manifold lines between the oven and the MS were heated to ~135 ºC to mitigate any volatile condensation in the lines before reaching the MS and also to reduce water background in the system. The Agilent EGA-MS system consists of a Frontier PY-3030 pyrolyzer attached to a 5975C inert XL mass spectrometer (MS). For analyses on this system, the pyrolyzer was initially held at 50 ºC for 5 min and flushed with helium then ramped at 35 ºC/min to 1050 ºC, under 30 mb of helium and a 0.5 sccm helium flow. Manifold lines were held at 135 ºC. Analog materials were either obtained from commercial sources (e.g., Sigma-Aldrich), from R. Morris at the NASA Johnson Space Center, or from the Clay Mineral Society Source Clays Repository. Several milligrams of <150 μm samples were weighed into sample cups and then loaded into one of the SAM-like EGA-MS systems for analysis (Table 1).

Key masses (represented as the mass-to-charge ratio, m/z) for both SAM analyses and SAM-like laboratory analyses were SO_2 (m/z 64, main mass and m/z 66, isotopologue), H_2S (m/z 34), OCS (m/z 60), CS_2 (m/z 76), H_2O (m/z 18, main mass and m/z 20, isotopologue), CO_2 (m/z 44, main mass and m/z 45, isotopologue), O_2 (m/z 32, main mass and m/z 34, isotopologue), CO and N_2 (m/z 28) and H_2 (the main

mass of H_2, m/z 2, was not monitored; but m/z 3 can represent H_2 (through HD or H^{3+})). The m/z representing the isotopologues were plotted in some cases because the main mass signal was saturated. Mass 34 can be attributed to H_2S, but m/z 34 can also result from the ^{34}S fragment of SO_2 and from an isotopologue of O_2 (i.e., $^{16}O^{18}O$). Consequently, the contribution of SO_2 fragments to the m/z 34 trace inferred from the SO_2 fragmentation pattern were subtracted from the signal; any residual m/z 34 signal was attributed to H_2S. The m/z 34 EGA traces did not track the EGA traces attributed to SO_2 (e.g., 64, 66) in some cases as would be expected if m/z 34 resulted dominantly from an SO_2 fragment. This observation also indicated that m/z 34 has significant contributions from a source other than SO_2 fragmentation. When a large oxygen peak was observed, such as near 400 ^oC in all of the Rocknest runs, the vast majority of m/z 34 coincident with the large O_2 peak results from the O_2 isotopologue ($^{16}O^{18}O$).

4. Results and Discussion

The EGA traces (e.g., Fig. 2 and Fig. 4) of Rocknest materials indicate evolution of SO_2, H_2S, OCS and CS_2 from approximately 450-800 ºC. The gas evolution traces vary between each Rocknest subsample run (discussed below). For SO_2 and H_2S, two peak evolutions were observed at ~500-550 °C and ~700-750 ºC, and the temperatures of the evolved H_2S trace peaks are systematically offset to higher temperatures as compared to the SO_2 peaks (Fig. 2) (Note: The peak in the m/z 34 trace near 400 ºC is not from H_2S but from the O_2 isotopologue ($^{16}O^{18}O$)).

Comparison of SAM SO_2 EGA traces with data collected on analog materials in SAM-like laboratory systems to date indicates that evolved SO_2 could result from the thermal decomposition of Fe-sulfates or Ca-sulfites, oxidation of sulfides, pyrolysis of organic sulfur compounds, and S adsorbed onto sample materials [*Clark*

and Baird, 1979] which can result in S-gas evolution at relatively high temperatures [*Rampe and Morris*, in prep], or a combination of these phases (Figure 3). Evolved H_2S could result from reaction of H_2O or H_2 with a reduced S-phase (e.g., pyrite or pyrrhotite) in the sample, or with evolved SO_2, or a combination of these.

The variations in abundances of SO_2 and H_2S evolved from each Rocknest subsample (Table 2) are likely due to heterogeneity in the amount of sulfur-bearing phase(s) between the different subsamples. The abundances of H_2O, CO_2, and O_2 consistently increased or decreased together across the four Rocknest runs indicating that differences in the mass of each Rocknest Scoop 5 subsample delivered to the SAM oven are responsible for these differences in abundance [*Archer et al.*, 2013a; *Glavin et al.*, 2013; *Leshin et al.*, 2013]). SO_2 and H_2S did not vary consistently with H_2O, CO_2, and O_2 abundances. These differences are not likely due to terrestrial volatiles within SAM as these species were not detected in the EGA blank run. In addition, there is no sulfur in the *N*-methyl-*N*-(*tert*-butyldimethylsilyl)trifluoroacetamide (MTBSTFA) (or significant fragments with m/z values overlapping those of SO_2), a vapor present in the SAM background at low pyrolysis temperatures (< ~500 ºC) that was derived from one of SAM's derivatization cups for wet chemistry experiments [*Glavin et al.*, 2013; *Leshin et al.*, 2013].

Some of the SO_2 is evolved from sulfur species associated with the ~30 wt % of X-ray amorphous (non-crystalline) material detected by the MSL Chemistry and Mineralogy (CheMin) X-ray diffraction (XRD) and X-ray fluorescence instrument in the Rocknest materials [*Bish et al.*, 2013]. If all evolved H_2S were attributed to the sulfides pyrite or pyrrhotite the implied abundance in the sample would be well below the expected CheMin mineral detection limit of ~1-2 wt% [*Bish et al.*, 2013], even for

the Rocknest run which evolved the most H_2S (Rocknest 3). For all Rocknest subsample runs other than perhaps Rocknest 1, however, if SO_2 were attributed to simple Fe-sulfate(s), the abundances of sulfate implied in a 50 mg sample delivered to SAM (e.g., for $FeSO_4$, ~3 to 7 wt%; for $Fe_2(SO_4)_3 \cdot 10H_2O$, ~4 to 9 wt%) would exceed the CheMin detection limit. Rocknest sulfates are most likely dominated by Fe-sulfates, but calculations for Mg and Ca sulfates would indicate the same general trend. A detailed search for sulfates in the Rocknest fines conducted by the CheMin team, including kieserite ($MgSO_4 \bullet H_2O$), szomolnokite ($Fe^{2+}SO_4 \bullet H_2O$), botryogen ($MgFe^{3+}(SO_4)_2(OH) \bullet 7(H_2O)$), jarosite ($KFe^{3+}{}_3(SO_4)_2(OH)_6$), rozenite ($Fe^{2+}SO_4 \bullet 4H_2O$), schwertmannite ($Fe^{3+}{}_{16}O_{16}(OH)_{12}(SO_4)_2$), and copiapite ($Fe^{2+}Fe^{3+}{}_4(SO_4)_6(OH)_2 \bullet 20(H_2O)$), showed no evidence that any sulfates other than anhydrite ($CaSO_4$) were present [*Bish*, 2013]. In addition, there is no evidence of intensity that could be attributed to a sulfate phase other than anhydrite; Rietveld refinement results shown in Figure 2 of *Bish et al.* [2013] illustrate this. Ca-sulfates such as anhydrite will not evolve SO_2 until temperatures higher than achieved by SAM analyses of Rocknest materials (>835 ºC). Because CheMin did not find crystalline sulfates expected to evolve SO_2 in the SAM temperature range [*Bish et al.*, 2013], another source for some of the evolved SO_2 is implied and the oxidation of a minor reduced sulfur phase could not account for all of it. Some SO_2 could evolve from sulfur species that are part of discrete X-ray amorphous sulfates or sulfites, or they could be adsorbed onto X-ray amorphous substrates such as Fe-allophane or nanophase iron oxide phases (npOx).

Small amounts of OCS and CS_2 were evolved from Rocknest fines (Table 2). These gases were evolved at temperatures approximately consistent with the higher temperature H_2S peak (Fig. 4). SO_2 and H_2S, as well as OCS and CS_2, released from

Rocknest were also identified by GCMS analyses (Fig. 5). Possible reactions occurring in the SAM oven during EGA-MS and the species that might be involved in these reactions are discussed below.

4.1 SO_2 evolved from Rocknest Fines

The ~500-550 ºC SO_2 peak in Rocknest data (Fig. 2, Fig. 3a) likely resulted in large part from the oxidation of a sulfide, such as pyrite or pyrrhotite. Rocknest soil fines evolved O_2 in the 300-500 ºC range (Fig. 2) and its source was attributed to the thermal decomposition of an oxychlorine phase(s) such as a perchlorate or chlorate salt [*Glavin et al.*, 2013; *Leshin et al.*, 2013]. The hypothesis that the SO_2 is largely from sulfide oxidation is consistent with the observation that the ~500-550 ºC SO_2 peak rises as the major O_2 peak drops off in the EGA traces from all four Rocknest runs (Fig. 2). Oxidation of a sulfide by evolved O_2 could be responsible for evolved SO_2 from Rocknest. Oxidation of the sulfides pyrite and pyrrhotite would result in the following reactions in the SAM oven [*Bhargava et al.*, 2009; *Hong and Fegley*, 1997b; *Hu et al.*, 2006]:

$2FeS_2 + 5\ ½\ O_2 \rightarrow Fe_2O_3 + 4SO_2$ (Eq. 1)

$3FeS_2 + 8O_2 \rightarrow Fe_3O_4 + 6SO_2$ (Eq. 2)

or

$2FeS + 3\ ½\ O_2 \rightarrow Fe_2O_3 + 2SO_2$ (Eq. 3)

$3FeS + 5O_2 \rightarrow Fe_3O_4 + 3SO_2$ (Eq. 4)

The production of hematite (Fe_2O_3) illustrated in Eqs. 1 and 3 is favored by higher O_2 concentrations in the gas above the sample and the production of magnetite (Fe_3O_4) shown in Eqs. 2 and 4 is favored by lower O_2 concentrations [e.g., *Hu et al.*, 2006].

To investigate the oxidation of sulfides with O_2 from perchlorates under SAM-relevant conditions, SAM-like laboratory analyses of sulfide and Ca-perchlorate

mixtures were carried out. Ca-perchlorate was chosen for these mixtures because it is currently thought to be the most likely candidate for the Rocknest perchlorate phase based on the temperature of O_2 release [*Glavin et al.*, 2013]. These analyses of Ca-perchlorate/pyrite mixtures and Ca-perchlorate/pyrrhotite mixtures exhibited a ~500-550 ºC peak in their SO_2 EGA trace with an onset temperature occurring at the end of the O_2 release (Eqns. 1-4 and 6) (Figs. 6 and 7). The evolved SO_2 from the pyrite/perchlorate and the pyrrhotite/perchlorate mixtures occurred at temperatures roughly consistent with Rocknest evolved SO_2. The SO_2 peak near 550 ºC may have resulted in part from oxidation of sulfide minerals with evolved O_2 from perchlorate via reactions shown in Eqns. 1-4 and 6.

Fe-sulfates, which have the lowest thermal decomposition temperatures of the common sulfates, generally evolve SO_2 at temperatures higher than the 500-550 ºC SO_2 peak observed in Rocknest (Fig. 3). It is possible however that nanophase Fe-sulfates may evolve SO_2 at lower temperatures [*Archer et al.*, 2013b; *Kotra et al.*, 1982; *Lauer et al.*, 2012]. Nanophases are consistent with the large quantity of X-ray amorphous materials in Rocknest materials detected by CheMin. However, if nanocrystalline Fe-sulfates are contributing to the lower temperature SO_2 at Rocknest, they likely do this in addition to contributions from a reduced sulfur phase. Laboratory evolved gas analyses of several Fe-sulfates (e.g., Figure 3b) do not evolve H_2S, suggesting that low temperature H_2S observed in Rocknest data is unlikely to be produced by the thermal decomposition of an Fe-sulfate phase.

Some oxidation of reduced S hosted in a sulfide, such as pyrite, could also occur through reactions with CO_2 that is present in the SAM pyrolysis oven near 550 ºC in Rocknest runs (Fig. 4) [e.g., *Bhargava et al.*, 2009]:

$$FeS_2 + 2CO_2 \rightarrow FeS + 2CO + SO_2 \qquad \text{(Eq. 5)}$$

This CO_2 is consistent with the thermal decomposition or acid dissolution (from reaction with gas phase HCl observed in Rocknest EGA, Fig. 2) of fine-grained or amorphous carbonates [*Archer et al.*, 2013b; *Cannon et al.*, 2012; *Sutter et al.*, 2012] that may be present as a result of the input of fine, global martian dust to the Rocknest materials (martian dust may contain 2-5 wt % Mg-carbonate [*Bandfield et al.*, 2003]). Fe-sulfates likely contribute at least some of the Rocknest evolved sulfur species (see discussion below), which implies the presence of acid solutions [e.g., *Bigham and Nordstrom*, 2000; *Jambor et al.*, 2000] in which carbonates would not form. If carbonates are eventually confirmed for Rocknest, this may indicate that Fe-sulfates do not contribute to the sulfur species evolved from Rocknest materials, and that other sources (eg., Ca-sulfites (Fig. 3b)) more likely contribute to the high temperature SO_2 peak. Alternatively, the Rocknest materials have experienced only minor, intermittent aqueous alteration and are in chemical disequilibrium.

SO_2 peaks were also observed near 700-750 ºC in the SAM-like laboratory analyses of sulfide/perchlorate mixtures, similar to the Rocknest ~700-750 ºC SO_2 evolution. Reduced sulfur phase(s) (e.g., pyrrhotite) could persist in the solid sample above ~550 ºC with incomplete oxidation, through reactions such as [*Bhargava et al.*, 2009; *Hu et al.*, 2006]:

$$FeS_2 + O_2 \rightarrow SO_2 + FeS \qquad \text{(Eq. 6)}$$

The amount of O_2 present near 750 ºC, both in Rocknest runs and in the SAM-like runs of simple sulfide/perchlorate mixtures, is very small, which makes the O_2 oxidation of reduced sulfur remaining in the oven to these temperatures a very minor potential contributor to the production of SO_2. It is possible in the case of Rocknest runs, however, that O_2 contributing to this reaction formed through other high temperature oven reactions suggested below for H_2S formation (mainly the reaction

shown in Eq. 13, which has O_2 as a product). In Rocknest runs (and sulfide/perchlorate laboratory runs) there is also very little CO_2 present near 750 ºC available for the reaction in Eq. 5 to produce SO_2.

Another possible contributor to the ~700-750 ºC SO_2 production in the Rocknest sample runs, and also in the laboratory pyrite/perchlorate and pyrrhotite/perchlorate runs, is the thermal decomposition of a Ca-sulfite product produced through the below reaction:

$$CaCl_2 + SO_2 + H_2O \rightarrow 2HCl + CaSO_3 \quad \text{(Eq. 7)}$$

The $CaCl_2$ is a product of the lower temperature thermal decomposition of Ca-perchlorate. This chloride could react with SO_2 to produce Ca-sulfite. As discussed below, and shown in Fig. 3b, Ca-sulfite would then thermally decompose to give SO_2 near 700 ºC.

Rocknest 1 shows a smaller amount of SO_2 evolved at ~700-750 ºC than the other 3 Rocknest runs. Oxidation of reduced S phases remaining in the oven to this temperature (e.g., FeS indigenous to the sample or formed as a product of the partial oxidation of FeS_2 (i.e., Eq. 5 and 6)) may be responsible for a significant amount of the ~700-750 ºC evolved SO_2 for Rocknest 1. Other sources of S for the ~700-750 ºC SO_2 are especially probable for the other Rocknest runs. The SO_2 could result from the thermal decomposition of a sulfate or sulfite mineral(s); Fe-sulfates and Ca-sulfites have high temperature SO_2 evolution peaks similar to Rocknest (Fig. 3). Thermal decomposition of these phases alone is not expected to also produce the ~700-750 ºC H_2S, however, indicating that another S-bearing material contributing to the high temperature S-gases may be present (e.g., sulfides) and/or that reactions are occurring between SO_2 and possible H_2 present in the oven at these temperatures, as discussed below.

SO_2 evolved from SO_4^{2-}-adsorbed on particle surfaces is also a candidate for the ~700-750 ºC SO_2 based on the large surface area available from the Rocknest X-ray amorphous materials for the adsorption of SO_4^{2-} and high temperature evolution of SO_2 expected from pyrolysis of materials such as SO_4^{2-} -adsorbed allophane and npOx [*Brydon and Singh*, 1969; *Rampe and Morris*, in prep]. Ca- and Mg-sulfates, including anhydrite detected in Rocknest by CheMin analyses [*Bish et al.*, 2013], have SO_2 evolution temperatures above the ~700-750 ºC Rocknest SO_2 evolution.

4.2 H_2S evolved from Rocknest Fines

The H_2S peak near 550 ºC could result from reaction of a sulfide such as pyrite or pyrrhotite with H_2O in the SAM ovens (Fig. 2) through reactions such as [e.g., *Hoare and Levy*, 1990]:

$$36FeS_2 + 22H_2O \rightarrow 22H_2S + 3Fe_{12}S_{13} + 11SO_2 \quad \text{(Eq. 8)}$$

Some of the Rocknest H_2S evolved near 750 ºC could also result from reactions with water in the oven at high temperature (Fig. 2), through reactions such as [e.g., *Hoare and Levy*, 1990; *Shao et al.*, 1994; *Uno*, 1951]:

$$FeS + H_2O \rightarrow H_2S + FeO \quad \text{(Eq. 9)}$$

$$3FeS + 4H_2O \rightarrow Fe_3O_4 + 3H_2S + H_2 \quad \text{(Eq. 10)}$$

SAM-like laboratory EGA analyses of a montmorillonite + pyrite mixture resulted in some H_2S evolved at temperatures consistent with the ~750 ºC evolution of H_2S from Rocknest samples (Fig. 9). This mixture was chosen because montmorillonite is known to evolve water (from dehydroxylation) at temperatures near 750 ºC, not because montmorillonite is known to be present in Rocknest samples. The amount of high temperature H_2S produced is small (Fig. 9), but similar to the amount of high temperature H_2S evolved from Rocknest 1 (Fig. 2). H_2S is also produced near 550 ºC during pyrolysis of the montmorillonite/pyrite mixture, probably through reactions

such as (Eq. 8). This H_2S evolution from the montmorillonite/pyrite mixure run is offset to slightly higher evolution temperatures as compared to the SO_2 peak, as observed in comparisons of the ~500-550 ºC SO_2 and H_2S peaks from Rocknest runs. Some of the ~750 ºC H_2S in Rocknest runs may have resulted from reaction of reduced S with the HCl [*Baba et al.*, 2011; *Ingraham et al.*, 1972]:

$FeS + 2HCl \rightarrow H_2S + FeCl_2$ (Eq. 11)

The production of high temperature HCl in Rocknest runs is detailed in *Glavin et al.,* [2013]. HCl could result from the reaction of Cl_2 produced by thermal decomposition of chlorides, either native to the sample or produced during thermal decomposition of a perchlorate salt, with H_2O. Another possible reaction is $CaCl_2$ reacting with evolved SO_2, O_2 and H_2O to form HCl and $CaSO_4$ through the Hargraves reaction:

$CaCl_2 + SO_2 + ½O_2 + H_2O \rightarrow 2HCl + CaSO_4$ (Eq. 12)

The abundance of any indigenous (i.e., not formed during pyrolysis from perchlorate), well-crystalline Cl-bearing phase in Rocknest soil fines is constrained to <1-2 wt % because greater abundances should have been detected by CheMin XRD analyses [*Bish et al.*, 2013].

H_2 evolved from Rocknest could also play a role in H_2S production. There is some evidence for the detection of H_2 evolving at very high temperatures during pyrolysis, which was not scavenged by reaction with SO_2 or other evolved volatiles (Fig. 2). The H_2 released at these high temperatures may have formed via reduction of H_2O.

If H_2 is produced, then it can react with SO_2 to form H_2S according to the following reaction [*Arutyunov et al.*, 1991; *Binns and Marshall*, 1991]:

$SO_2 + H_2 \rightarrow H_2S + O_2$ (Eq. 13)

The yield of H_2S from this reaction should generally depend on the initial H_2/SO_2 ratio. H_2S formation is promoted by increasing excess of H_2 [*Arutyunov et al.*, 1991]. *Arutynunov et al.* [1991] stated that there is an induction period in this reaction, such that the reaction rate is slow at first and increases with time. The delay in the high temperature H_2S release in Rocknest runs, and in laboratory runs, compared to the high temperature SO_2 release could result from this effect.

4.3 OCS and CS_2 evolved from Rocknest Fines

OCS and CS_2 evolved near 750 ºC in Rocknest runs (Fig. 4) could result from reactions of H_2S with CO_2, CO, or reduced C, or reactions between sulfides (e.g., FeS_2) and CO_2, CO, or reduced C, or a combination of these processes. There was CO, and very small amounts of CO_2, evolved near 750 ºC during Rocknest runs (Figs. 4 and 8).

The high temperature OCS could result from gas phase reactions, such as [*Gargurevich*, 2005; *Shao et al.*, 1994]:

$$H_2S + CO \rightarrow OCS + H_2 \qquad \text{(Eq. 14)}$$

or

$$H_2S + CO_2 \rightarrow OCS + H_2O \qquad \text{(Eq. 15)}$$

Gas-solid reactions may also occur in the SAM oven, e.g., reactions such as [*Bhargava et al.*, 2009; *Hong and Fegley*, 1997a; *Shao et al.*, 1994]:

$$FeS_2 + CO \rightarrow OCS + FeS \qquad \text{(Eq. 16)}$$

or

$$3FeS_2 + 4CO_2 + 2CO \rightarrow Fe_3O_4 + 6OCS \qquad \text{(Eq. 17)}$$

OCS production on Venus has been postulated to result from these types of thermochemical reactions; OCS is the second most abundant sulfur gas after SO_2 observed in the lower atmosphere [e.g., *Hong and Fegley*, 1997a].

CS_2 evolved near 750 ^oC in Rocknest data could be produced by reaction of OCS with H_2S [*Shao et al.*, 1994]:

e.g., $OCS + H_2S \rightarrow CS_2 + H_2O$ (Eq. 18)

The CO, and CO_2, in these reactions could result from the decomposition of very small amounts of carbonate at high temperature (e.g., calcite) or, possibly, from partial fragmentation/oxidation of refractory organic carbon compounds. The abundance of carbon in the $OCS + CS_2$ evolved from Rocknest subsamples (abundances in Table 2) is equivalent to ~0.4 to 1 ppm carbon. If all of this carbon initially resulted from calcite decomposition, because the CO and CO_2 involved in the reactions above result from calcite decomposition, it would indicate ~0.0003 – 0.0012 wt % calcite. The presence of this small amount of calcite in a sample of martian surface fines is reasonable [e.g., *Gooding*, 1978], especially given the likely presence of a carbonate phase responsible for some of the large, lower temperature CO_2 releases from Rocknest [*Archer et al.*, 2013a]. It is also possible the ~0.4 – 1 ppm carbon originated from refractory organic compounds, because all the CO and CO_2 involved in the reactions above originates from the heating of these organic compounds or because reduced organic C was incorporated into the CS_2 or OCS.

Refractory organic macromolecules are observed as the predominant organic component of carbonaceous chondrites and interplanetary dust particles (IDPs) and in some cases are associated with sulfates and sulfides, such as pyrrhotite ($Fe_{(1-x)}S$) [*Gibson*, 1992; *Sephton*, 2012; *Zega et al.*, 2010]. Some martian meteorites also contain macromolecular carbon indigenous to the mafic mineral assemblage hosting it [*Sephton et al.*, 2002; *Steele et al.*, 2013; *Steele et al.*, 2012], and in some cases this macromolecular carbon is associated with sulfide grains [*Steele et al.*, 2012]. Because of their refractory nature [e.g., *Steele et al.*, 2012], these materials might not

decompose until temperatures near the highest that the SAM oven can achieve, if at all. Their decomposition could be facilitated by thermochemical reactions between solids or gases within the pyrolysis oven at high temperature. Refractory organic material could also facilitate reactions, such as thermochemical reduction of sample sulfates [*Xu et al.*, 2004; *Zhang et al.*, 2012; *Zhang et al.*, 2008; *Zhang et al.*, 2007]. If these processes involving reduced organic carbon occurred at the high temperatures at which several reduced S-gases are evolved from Rocknest, they could contribute to the CS_2 and OCS production, as well as possibly the H_2S production.

An important consideration is that mass spectra for reduced carbon bearing gases evolving coincidentally with CS_2 and OCS have not been observed in Rocknest EGA [*Leshin et al*., 2013]. In addition, the only organic compounds revealed by GCMS data are also detected in blank analyses and are likely associated with the SAM instrument background, though a contribution from martian carbon to these compounds can not be excluded [*Glavin et al.*, 2013]. However, it is possible that any small amounts of carbon that were evolved from partial high temperature decomposition of refractory organic compounds in the Rocknest sample were "scrubbed" by reaction with sulfur-bearing gases, or were evolved as CO or CO_2, thus preventing unequivical detection of high temperature organic fragments in EGA or GCMS. The ppm levels of carbon would be well within the concentration of organic carbon that might be expected in martian surface materials based on martian meteorite analyses that examined indigenous martian organic carbon (1 ppm to several hundred ppm [e.g., *Grady et al.*, 2004; *Jull et al.*, 2000; *Steele et al.*, 2012; *Steininger et al.*, 2012] or resulting from exogenous meteoritic input (up to ~60 ppm [*Steininger et al.*, 2012]), or both.

5. Implications

5.1 Evidence for Minor Crystalline Sulfur Phases and Sulfur-bearing Amorphous Material

The few weight percent SO_3 (0.5-3.7 wt %) inferred from EGA data (Table 2) is a substantial fraction of the total SO_3 measured by APXS at Rocknest (5.45 ± 0.10 wt %, location Portage [*Blake et al.*, 2013], Fig. 1), consistent with the hypothesis that, in addition to the Ca-sulfate detected by CheMin [*Bish et al.*, 2013], Rocknest contains other S-bearing phases. APXS analyzed Rocknest soil fines, equivalent to those analyzed by SAM and CheMin, which had been sieved to <150 μm by CHIMRA and dumped on the MSL Ti observation tray (o-tray). Although it was not possible to obtain quantitative elemental abundances from this APXS o-tray measurement because the sample was too thin and covered only part of the APXS field of view, the analyses indicated a slightly elevated S content compared with the bulk Rocknest materials analyzed by APXS at Portage [*Berger et al.*, 2013]. The enrichment of S-bearing materials in the finer fraction examined on the observation tray is likely due to some concentration of martian dust and/or soil alteration products.

The only crystalline sulfur-bearing phase identified by CheMin analysis was the mineral anhydrite ($CaSO_4$), which generally decomposes at temperatures higher than those achievable by SAM (>835 ºC). CheMin also revealed a significant (~30 wt%) X-ray amorphous soil component [*Bish et al.*, 2013]. Together, these observations imply that the phases hosting the sulfur evolved during SAM analysis were minor abundances of crystalline sulfur phases such as sulfates, sulfites or sulfides present below CheMin detection limits (<1-2 wt%), or were in an X-ray amorphous phase. For crystalline phases present below the CheMin detection limits, SAM-like laboratory data to date indicate that SAM sulfur-species EGA data from Rocknest is most consistent with Fe-sulfates, Ca-sulfites and sulfides such as pyrite or

pyrrhotite. Mass balance calculations from CheMin and APXS data suggest that X-ray amorphous phases incorporate a significant amount of the sulfur (~4.9 wt % SO_3) [*Blake et al.*, 2013].

Prime candidates for the amorphous component, based on calculations from Rocknest APXS measurements (Portage) and comparison with MER soil APXS datasets [*Blake et al.*, 2013; *Morris et al.*, 2013], as well as on orbital observations [e.g., *Kraft et al.*, 2003; *Michalski et al.*, 2006; *Milliken et al.*, 2008], terrestrial analog [e.g., *Morris et al.*, 2000], laboratory [e.g., *Hurowitz et al.*, 2006] and martian meteorite studies [e.g., *Gooding and Muenow*, 1986], are amorphous and poorly crystalline aluminosilicate and/or silica-rich materials, and X-ray amorphous npOx materials. A poorly crystalline phase resembling hisingerite ($Fe_2Si_2O_5(OH)_4 \bullet 2H_2O$) or Fe-allophane has also been suggested by the elevated low-angle background in the CheMin XRD pattern from Rocknest soil fines [*Bish et al.*, 2013].

The sulfate ion is known to adsorb onto allophane and npOx materials, such that SO_2 should be released upon heating to high temperatures including temperatures higher than achievable by SAM's Oven #1 [*Rampe and Morris*, in prep] (SAM has two pyrolysis ovens, Oven #2 can achieve higher sample temperatures (>~1050-1100 ºC) [*Mahaffy et al.*, 2012] but was not available for use during the Rocknest campaign). Preliminary work with SAM-like EGA of synthetic SO_4^{2-}-adsorbed allophane and SO_4^{2-}-adsorbed npOx samples by *Rampe and Morris* [in prep] has shown that SO_2 can evolve over a range of high temperatures including temperatures above the SAM Oven #1 temperature range and work is ongoing. The idea that a fraction of the Rocknest fines' total sulfur is associated with an X-ray amorphous phase that also does not decompose in the SAM temperature range is consistent with a comparison of APXS, CheMin and SAM data from Rocknest fines. If SAM-derived

SO_3 abundances (~2 wt % average) and CheMin-derived SO_3 abundances (~0.9 wt % SO_3 from 1.5 wt% anhydrite [*Bish et al.*, 2013]) from Rocknest are subtracted from the 5.45 wt % SO_3 from APXS analysis of Rocknest material (Portage), ~2.6 wt % SO_3 remains. This remaining SO_3 could either result from small abundances of a sulfate (below CheMin detection limits) that evolves SO_2 at temperatures above the temperatures of SO_2 evolution from Rocknest or be associated with an X-ray amorphous phase that does not evolve SO_2 in the SAM temperature range. The adsorption of sulfate onto iron oxides and other soil components is well known in several environments on Earth [e.g., *Aylmore et al.*, 1967; *Parfitt and Smart*, 1978]. Mars, with its proposed S-rich alteration environment [e.g., *Gaillard et al.*, 2013; *Halevy et al.*, 2007; *Johnson et al.*, 2008; *King and McLennan*, 2010; *King and McSween*, 2005; *McLennan*, 2012; *McLennan and Grotzinger*, 2008] and ubiquitous fine-grained Fe-rich material may be comparatively more likely to have S-anions adsorbed onto those phases in soil materials.

5.2 Reduced and Oxidized Sulfur Phases and the Provenance of Rocknest Material

The presence of sulfate minerals in Rocknest materials suggests aqueous alteration either intrinsic to the Rocknest deposit or in the formation environment of the sulfate minerals that ultimately accumulated in the deposit (i.e., S-bearing materials were formed by alteration elsewhere and transported to the Rocknest site by wind). Of the common sulfates, SAM EGA SO_2 traces from Rocknest materials are most consistent with SO_2 release resulting from the thermal decomposition of Fe-sulfates (Fig. 3). Prior landing sites have shown evidence for Mg-sulfates as the dominant S-bearing phase in soils [*Kounaves et al.*, 2010; *Vaniman et al.*, 2004] but those measurements were made mostly at sites in the northern lowlands. The older southern highlands may have different and more diverse S speciation, as seen at

Rocknest and supported by Spirit's results from the Columbia Hills, where soils with acid Fe-sulfates (and lesser Ca-sulfates) were found along with possible excess S in non-sulfate phases [*Arvidson et al.*, 2010; *Yen et al.*, 2008]. In addition, global elemental correlations of gamma-ray spectroscopy data suggest that Fe-sulfates may be a key hydrous phase in bulk martian soil at decimeter depths [*Karunatillake et al.*, 2012]. Fe-sulfates in Rocknest materials are consistent with acid interactions with martian surface materials, because these sulfates generally precipitate in acid conditions. The minor abundance of these sulfates in Rocknest materials, and the possible presence of minor carbonates, suggests a physical mixture of Fe-sulfate and carbonate. Distal acid-altered deposits [e.g., *Niles and Michalski*, 2009; *Squyres and Knoll*, 2005; *Wray et al.*, 2011] could have eroded, and particles subsequently transported by wind to the Rocknest site where Fe-sulfate was physically mixed with carbonate. Alternatively, Fe-sulfate was formed in low water-to-rock ratio (W/R) settings within the Rocknest materials such that carbonate was not completely dissolved. These low W/R settings could involve interactions of acid aerosols with Fe-bearing basalt components such as olivine, pyroxenes or glass [*Tosca et al.*, 2004] or alteration of Fe-bearing basaltic materials by acidic thin water films near sulfide grains [*Chevrier and Mathe*, 2007].

Gale Crater's Mt. Sharp is unlikely to be the only source of sulfates based on the orbital remote sensing evidence for Mg-dominated sulfates in its relatively dust-free strata [*Milliken et al.*, 2010]. It is possible however that some Mt. Sharp-derived Mg-sulfate grains, which would be relatively water soluble, were transported by wind to the Rocknest site. There they may have been dissolved in small amounts of water that also contained other cations from basalt dissolution (e.g., Fe, Ca, etc.) and sulfates of these other cations were precipitated. Solubility relationships indicate that

sulfates of these other cations could precipitate ahead of Mg-sulfates during evaporation [e.g., *Lindsay*, 1979].

Sulfites, if present, could imply the oxidation of reduced sulfur but under conditions that did not allow oxidation to sulfate [*Chevrier et al.*, 2012]. Sulfites would also imply that the Rocknest materials have experienced very little interaction with liquid water since their formation because they would readily oxidize to sulfates in the presence of water [*Halevy and Schrag*, 2009; *Halevy et al.*, 2007; *Marion et al.*, 2013]. There is also the possibility that sulfites could form by the irradiation of sulfates in the martian surface environment [*Luo et al.*, 1998; *Tani et al.*, 2012]. In this case, the Rocknest Ca-sulfates could serve as the precursor to Ca-sulfite formation; Ca-sulfites evolve high temperature SO_2 at temperatures consistent with Rocknest (Fig. 3). Alternatively, surface sulfite minerals have been hypothesized to form during an early martian climate feedback involving the outgassing of SO_2 and H_2S as a result of volcanic activity [*Halevy and Schrag*, 2009; *Halevy et al.*, 2007; *Marion et al.*, 2013]. These authors specifically point to the likelihood of precipitation of Ca-sulfite instead of calcite or Ca-sulfate at acidic to near-neutral pHs. This is because SO_2 is more soluble than CO_2 and because sulfurous acid is a stronger acid than carbonic acid leading to the majority of sulfur in solution present as the sulfite anion while very little carbon occurs as the carbonate anion. In the presence of iron, however, siderite (and also secondary silicates such as phyllosilicates) can be expected to precipitate together with the Ca-sulfite [*Halevy and Schrag*, 2009; *Halevy et al.*, 2007]. Later interactions with water and a more oxidizing martian atmosphere could allow some oxidation of these sulfites to sulfates [*Halevy and Schrag*, 2009; *Halevy et al.*, 2007; *Marion et al.*, 2013]. These studies suggest that any Ca-sulfite in Rocknest materials could have precipitated together

with an iron carbonate and could have been partially oxidized to form some of the Ca-sulfates found in Rocknest materials by CheMin.

Some Rocknest sulfur phases are most likely locally derived. SAM EGA data suggest the presence of sulfides, i.e., pyrite or pyrrhotite, in Rocknest. It is likely that sulfides are igneous, have been physically weathered from local sulfide-bearing basalt sources (martian basalts have as much as 1% sulfide mineralogy [*Chevrier et al.*, 2011; *Lorand et al.*, 2005; *McCoy et al.*, 1992]) and transported by aeolian processes to their current residence in the Rocknest deposit. Sulfides in the Rocknest fines could also indicate some contributions from sedimentary materials originally deposited in a reducing environment. Evidence for a reducing environment could be an important consideration for finding and detecting organic compounds, as reducing environments are more favorable for organic preservation [*Killops and Killops*, 2005; *Summons et al.*, 2011]. Even if sulfides just occur in the Rocknest soil because of the physical weathering of basalt rocks, or because of the input of some sulfide-bearing exogenous meteoritic material (or both), their presence implies that the Rocknest area has been relatively dry since the sulfides were incorporated into the deposit. In the presence of water, the sulfides would oxidize to produce sulfate anions (Eq. 19) [e.g., *Burns and Fisher*, 1990; *Jambor et al.*, 2000; *Zolotov and Shock*, 2005].

$$FeS_2 + 8H_2O \rightarrow Fe^{2+} + 2SO_4^{2-} + 2H^+ + 7H_2 \qquad \text{(Eq. 19)}$$

These could react with cations available in solution from alteration of nearby basaltic materials to form sulfates [e.g., *Burns and Fisher*, 1990; *Jambor et al.*, 2000; *Zolotov and Shock*, 2005]. The presence of dissolved O_2 facilitates this reaction (Eq. 20), and even thermodynamic modeling with solutions having the low fO_2 resulting from equilibrium with the current martian atmosphere indicate pyrite dissolution/oxidation could be expected to occur via reaction shown in Eq. 20 [*Zolotov and Shock*, 2005].

$FeS_2 + 3.5O_2(aq) + H_2O \rightarrow Fe^{2+} + 2SO_4^{2-} + 2H^+$ (Eq. 20)

The susceptibility of sulfides to alteration/oxidation implies that they were derived from local rocks and then not subsequently subjected to significant aqueous alteration, although it is possible the sulfides were incorporated within transported regional or global basaltic materials such that alteration was unable to penetrate fully into the sulfide-containing part of the grain during transport.

The OCS and CS_2 evolved from Rocknest materials likely result from reactions between reduced sulfur phases such as sulfides and CO_2, CO or reduced carbon at high temperature. CO_2 or CO could originate from decomposition of trace calcite and CO_2, CO or reduced C could result from partial decomposition of high temperature organic compounds. Although no unequivocal EGA or GCMS evidence for martian reduced carbon bearing gases evolved coincidentally with the CS_2 and OCS was obtained [*Leshin et al.*, 2013; *Glavin et al*., 2013], it is possible that any small amounts of reduced C from partial decomposition of refractory organic compounds were incorporated into OCS or CS_2, or were evolved as CO or CO_2. In addition, the very small amounts of C implied by the OCS and CS_2 detected (≤ ~1 ppm) are below that which could be expected from estimates of indigenous martian or exogeneous meteoritic carbon (1 ppm to several hundred ppm [e.g., *Grady et al.*, 2004; *Jull et al.*, 2000; *Steele et al.*, 2012; *Steininger et al.*, 2012]). Consequently, a possible contribution of reduced organic carbon to the CS_2 and OCS detected from Rocknest cannot be excluded and ongoing investigations of materials at Gale may allow further insight into the presence and nature of reduced organic carbon in martian surface materials.

Even if sulfides play a key role in both SO_2 peaks in SAM EGA data, CheMin data indicate the presence of Ca-sulfates; thus there is a high likelihood of both

reduced and oxidized sulfur compounds in the Rocknest soil deposit. Sulfites would represent an oxidation state of sulfur (S^{4+}) intermediate between that of sulfur in sulfides (e.g., FeS (S^{2-})) and sulfates (S^{6+}). This heterogeneity in sulfur oxidation states within the components of the deposit indicates a non-equilibrium assemblage. This disequilibrium assemblage could possibly have implications for the habitability of Rocknest materials since the metabolisms of some terrestrial microbes are known to exploit redox gradients for energy [e.g., *Jakosky and Shock*, 1998; *Summons et al.*, 2011]. Evidence that the Rocknest materials have not achieved chemical equilibrium is consistent with the well-supported hypothesis that martian surface environments have been dry for the past several billion years [e.g., *Bibring et al.*, 2006; *Carr*, 1987], a timeframe that probably easily encompasses the age of the Rocknest deposit [*Blake et al.*, 2013].

6. Summary

Fines from the Rocknest deposit likely contain both reduced and oxidized sulfur-bearing phases. SAM pyrolysis resulted in the evolution of both oxidized and reduced sulfur compounds, including SO_2, H_2S, OCS, and CS_2. These data represent the first time sulfur species have been detected during *in situ* pyrolysis of martian surface material. EGA traces show a wide temperature range of SO_2 and H_2S evolution within which there are peaks in intensity near 500-550 ºC and near 700-750 ºC. SO_2 is likely produced by thermal decomposition of Fe-sulfates or Ca-sulfites, evolved/desorbed from sulfur-bearing amorphous phases, and produced by reactions between reduced sulfur phases and O_2 or H_2O. H_2S is likely produced from the interaction of evolved H_2O, H_2 and/or HCl with reduced sulfur in the SAM oven, and/or produced from the reaction of SO_2 and H_2. OCS and CS_2 are probably

products of reactions involving a carbon source such as CO_2, CO or reduced carbon and reduced sulfur at high temperature.

The only crystalline sulfur-bearing phase identified by CheMin XRD analysis of Rocknest fines was anhydrite ($CaSO_4$), which generally decomposes at temperatures higher than the SAM temperature range. The weight percent of SO_3 inferred from Rocknest evolved SO_2, as well as that derived from APXS analyses of Rocknest materials, indicates the presence of other sulfur-bearing phases, but they must be present below the CheMin detection limit or are non-crystalline. CheMin also revealed a significant X-ray amorphous component in the Rocknest soil. SAM EGA-derived total evolved SO_2 and EGA traces consistent with sulfide and sulfate/sulfite sample phases, together with CheMin detection of a significant amorphous component, imply that the phases hosting the sulfur evolved during SAM analysis were minor amounts of crystalline sulfur phases including sulfides and sulfates/sulfites present below CheMin detection limits and an X-ray amorphous phase.

The complex sulfur-bearing phase assemblage is consistent with the derivation of Rocknest material from a combination of local, regional, and global sources as suggested by a synthesis of MSL Rocknest datasets [*Blake et al.*, 2013], but it is also consistent with an origin of Rocknest materials from the weathering of local rocks with complex formation/alteration histories. Sulfate-rich bedrock has been observed in several regions on Mars [*Baldridge et al.*, 2013; *Milliken et al.*, 2010; *Squyres and Knoll*, 2005; *Wray et al.*, 2011; *Wray et al.*, 2009], and as invoked for those settings, sulfates in the Rocknest fines indicate aqueous alteration processes. This alteration may have occurred elsewhere before incorporation of the sulfates into the Rocknest deposit or within the deposit, or a combination of these. Of the common sulfates, the

SAM EGA data are most consistent with Fe-sulfates. Because Fe-sulfates generally form in acidic aqueous environments, their presence indicates either acid alteration within the Rocknest deposit, or alteration elsewhere followed by transport of materials to the Rocknest site. SO_2 evolved from sulfite minerals, such as Ca-sulfite, is also a possible contributor and Ca-sulfite is consistent with acidic to near-neutral aqueous alteration settings. Sulfides such as pyrite or pyrrhotite in the Rocknest fines likely indicate contributions from materials weathered from basaltic parent rocks, or materials originally deposited in a reducing environment. The susceptibility of sulfides to alteration/oxidation implies that they were likely derived from local rocks. The possibility of sulfur compounds with a range of sulfur oxidation states together in the Rocknest deposit, a non-equilibrium assemblage, supports the common assertion that martian surface environments have been dry for the probable geologically short age of the Rocknest bedform [*Blake et al.*, 2013], and likely for the past several billion years.

Acknowledgements

NASA provided support for the development of SAM. Data from these SAM experiments will be archived in the Planetary Data System (pds.nasa.gov) in 2013. Essential contributions to the successful operation of SAM on Mars and the acquisition of SAM data were provided by the SAM development, operations, and testbed teams. P.D.A. and C.F. acknowledge support from the NASA Postdoctoral Program, administered by Oak Ridge Associated Universities through a contract with NASA. We thank members of the SAM and larger MSL team for insightful discussions and support. We also thank Melissa Lane and two anonymous reviewers for helpful comments.

References

Anderson, R. C., et al. (2012), Collecting Samples in Gale Crater, Mars; an Overview of the Mars Science Laboratory Sample Acquisition, Sample Processing and Handling System, *Space Science Reviews*, *170*(1-4), 57-75, doi:10.1007/s11214-012-9898-9.

Archer, P. D., et al. (2013a), Abundances and implications of volatile-bearing species from Evolved Gas Analysis of the Rocknest aeolian bedform, Gale Crater, Mars, *Journal of Geophysical Research Planets*, accepted.

Archer, P. D., D. W. Ming, and B. Sutter (2013b), The effects of instrument parameters and sample properties on thermal decomposition: interpreting thermal analysis data from Mars, *Planetary Science*, *2*(21), doi:10.1186/2191-2521-1182-1182.

Arutyunov, V. S., V. Y. Basevich, V. I. Vedeneev, O. V. Sokolov, V. A. Ushakov, and A. V. Chernysheva (1991), Kinetics Of The Reduction Of Sulfur-Dioxide .3. Formation Of Hydrogen-Sulfide In The Reaction Of Sulfur-Dioxide With Hydrogen, *Kinetics and Catalysis*, *32*(5), 1112-1115.

Arvidson, R. E., et al. (2010), Spirit Mars Rover Mission: Overview and selected results from the northern Home Plate Winter Haven to the side of Scamander crater, *Journal of Geophysical Research-Planets*, *115*, doi:10.1029/2010je003633.

Aylmore, L. A. G., M. Karim, and J. P. Quirk (1967), Adsorption and Desorption of Sulfate Ions by Soil Constituents, *Soil Science*, *103*(1), 10-15.

Baba, A. A., F. A. Adekola, O. O. Opaleye, and R. B. Bale (2011), Dissolution Kinetics Of Pyrite Ore By Hydrochloric Acid, *Journal of Applied Science and Technology*, *16*, 104-110.

Baker, L. L., D. J. Agenbroad, and S. A. Wood (2000), Experimental hydrothermal alteration of a martian analog basalt: Implications for martian meteorites, *Meteoritics & Planetary Science*, *35*(1), 31-38.

Baldridge, A. M., M. D. Lane, and C. S. Edwards (2013), Searching at the right time of day: Evidence for aqueous minerals in Columbus crater with TES and THEMIS data, *Journal of Geophysical Research Planets*, *118*, 179-189.

Bandfield, J. L., T. D. Glotch, and P. R. Christensen (2003), Spectroscopic identification of carbonate minerals in the martian dust, *Science*, *301*(5636), 1084-1087.

Banin, A., F. X. Han, I. Kan, and A. Cicelsky (1997), Acidic volatiles and the Mars soil, *Journal of Geophysical Research-Planets*, *102*(E6), 13341-13356.

Benison, K. C., and D. A. Laclair (2003), Modern and ancient extremely acid saline deposits: Terrestrial analogs for martian environments?, *Astrobiology*, *3*(3), 609-618, doi:10.1089/153110703322610690.

Berger, J. A., P. L. King, R. Gellert, J. L. Campbell, N. Boyd, I. Pradler, G. M. Perrett, APXS, and MSL Teams (2013), MSL Titanium Observation Tray Measurements with APXS, in *LPI Contribution No. 1719,* p.1321, Lunar and Planetary Institute, Houston.

Bhargava, S. K., A. Garg, and N. D. Subasinghe (2009), In situ high-temperature phase transformation studies on pyrite, *Fuel*, *88*(6), 988-993, doi:10.1016/j.fuel.2008.12.005.

Bibring, J. P., et al. (2007), Coupled ferric oxides and sulfates on the Martian surface, *Science*, *317*(5842), 1206-1210, doi:10.1126/science.1144174.

Bibring, J. P., et al. (2006), Global mineralogical and aqueous mars history derived from OMEGA/Mars express data, *Science*, *312*(5772), 400-404, doi:10.1126/science.1122659.

Biemann, K., et al. (1976), Search For Organic And Volatile Inorganic-Compounds In 2 Surface Samples From Chryse-Planitia Region Of Mars, *Science*, *194*(4260), 72-76, doi:10.1126/science.194.4260.72.

Bigham, J. M., and D. K. Nordstrom (2000), Iron and Aluminum Hydroxysulfates from Acid Sulfate Waters in *Sulfate Minerals: Crystallography, Geochemistry, and Environmental Significance*, edited by C. N. Alpers, Jambor, J. L., Nordstrom, D. K., pp. 351-403, The Mineralogical Society of America, Washington D.C.

Binns, D., and P. Marshall (1991), An Abinitio Study Of The Reaction Of Atomic-Hydrogen With Sulfur-Dioxide, *Journal of Chemical Physics*, *95*(7), 4940-4947, doi:10.1063/1.461710.

Bish, D. L. (2013), personal communication.

Bish, D. L., et al. (2013), X-ray Diffraction Results from Mars Science Laboratory: Mineralogy of Rocknest at Gale Crater, *Science*, *341*(6153), doi:10.1126/science.1238932.

Bish, D. L., and C. J. Duffy (1990), Thermogravimetric Analysis of Minerals, in *Thermal Analysis in Clay Science* edited by J. W. Stucki, D. L. Bish and F. A. Mumpton, The Clay Minerals Society, Boulder, Colorado.

Bishop, J. L., et al. (2009), Mineralogy of Juventae Chasma: Sulfates in the light-toned mounds, mafic minerals in the bedrock, and hydrated silica and hydroxylated ferric sulfate on the plateau, *Journal of Geophysical Research-Planets*, *114*, doi:10.1029/2009je003352.

Blake, D. F., et al. (2013), Curiosity at Gale Crater, Mars: Characterization and Analysis of the Rocknest Sand Shadow, *Science*, *341*(6153), doi:10.1126/science.1239505.

Bridges, J. C., D. C. Catling, J. M. Saxton, T. D. Swindle, I. C. Lyon, and M. M. Grady (2001), Alteration assemblages in martian meteorites: Implications for near-surface processes, *Space Science Reviews*, *96*(1-4), 365-392.

Bruckner, J., G. Dreibus, R. Rieder, and H. Wanke (2003), Refined data of Alpha Proton X-ray Spectrometer analyses of soils and rocks at the Mars Pathfinder site: Implications for surface chemistry, *Journal of Geophysical Research-Planets*, *108*(E12), doi:10.1029/2003je002060.

Brydon, J. E., and S. S. Singh (1969), The Nature of the Synthetic Crystalline Basic Aluminum Sulfates as Compared with Basaluminite, *Canadian Mineralogist*, *9*, 644-654.

Burns, R. G., and D. S. Fisher (1990), Iron-Sulfur Mineralogy Of Mars - Magmatic Evolution And Chemical-Weathering Products, *Journal of Geophysical Research-Solid Earth and Planets*, *95*(B9), 14415-14421, doi:10.1029/JB095iB09p14415.

Cannon, K. M., B. Sutter, D. W. Ming, W. V. Boynton, and R. Quinn (2012), Perchlorate induced low temperature carbonate decomposition in the Mars Phoenix Thermal and Evolved Gas Analyzer (TEGA), *Geophysical Research Letters*, *39*, doi:10.1029/2012gl051952.

Carr, M. H. (1987), Water On Mars, *Nature*, *326*(6108), 30-35, doi:10.1038/326030a0.

Charsley, E. L., N. J. Manning, and S. B. Warrington (1987), A New Integrated System For Simultaneous TG-DTA-Mass Spectrometry, *Thermochimica Acta*, *114*(1), 47-52, doi:10.1016/0040-6031(87)80239-3.

Chevrier, V., J. P. Lorand, and V. Sautter (2011), Sulfide petrology of four nakhlites: Northwest Africa 817, Northwest Africa 998, Nakhla, and Governador Valadares,

Meteoritics & Planetary Science, *46*(6), 769-784, doi:10.1111/j.1945-5100.2011.01189.x.

Chevrier, V., and P. E. Mathe (2007), Mineralogy and evolution of the surface of Mars: A review, *Planetary and Space Science*, *55*(3), 289-314.

Chevrier, V. F., E. Dehouck, C. G. Lozano, and T. S. Altheide (2012), Mineral Parageneses Resulting from Weathering on Early Mars and the Effect of CO_2 vs SO_2 Atmospheres, in *LPI Contribution No. 1680,* id.7080, Lunar and Planetary Institute, Houston.

Clark, B. C., and A. K. Baird (1979), Is The Martian Lithosphere Sulfur Rich, *Journal of Geophysical Research*, *84*, 8395-8403, doi:10.1029/JB084iB14p08395.

Clark, B. C., A. K. Baird, H. J. Rose, P. Toulmin, K. Keil, A. J. Castro, W. C. Kelliher, C. D. Rowe, and P. H. Evans (1976), Inorganic Analyses of Martian Surface Samples at Viking Landing Sites, *Science*, *194*(4271), 1283-1288.

Clark, B. C., A. K. Baird, R. J. Weldon, D. M. Tsusaki, L. Schnabel, and M. P. Candelaria (1982), Chemical-Composition of Martian Fines, *J. Geophys. Res.*, *87*(NB12), 59-67.

Clark, B. C., and D. C. Vanhart (1981), The Salts of Mars, *Icarus*, *45*(2), 370-378.

Dyar, M. D., et al. (accepted), Mössbauer parameters of sulfate minerals, *American Mineralogist*.

Farrand, W. H., T. D. Glotch, J. W. Rice, J. A. Hurowitz, and G. A. Swayze (2009), Discovery of jarosite within the Mawrth Vallis region of Mars: Implications for the geologic history of the region, *Icarus*, *204*(2), 478-488, doi:10.1016/j.icarus.2009.07.014.

Franz, H. B., P. R. Mahaffy, W. Kasprzak, E. Lyness, and E. Raaen (2011), Measuring Sulfur Isotope Ratios from Solid Samples with the Sample Analysis at

Mars Instrument and the Effects of Dead Time Corrections, in *Contribution No. 1608,* p.2800, Lunar and Planetary Institute, Houston.

Gaillard, F., J. Michalski, G. Berger, S. M. McLennan, and B. Scaillet (2013), Geochemical Reservoirs and Timing of Sulfur Cycling on Mars, *Space Science Reviews*, *174*(1-4), 251-300, doi:10.1007/s11214-012-9947-4.

Gargurevich, I. A. (2005), Hydrogen sulfide combustion: Relevant issues under Claus furnace conditions, *Industrial & Engineering Chemistry Research*, *44*(20), 7706-7729, doi:10.1021/ie0492956.

Gellert, R., et al. (2006), Alpha particle X-ray spectrometer (APXS): Results from Gusev crater and calibration report, *Journal of Geophysical Research-Planets*, *111*(E2), doi:10.1029/2005je002555.

Gendrin, A., et al. (2005), Sulfates in martian layered terrains: the OMEGA/Mars Express view, *Science*, *307*(5715), 1587-1591.

Gibson, E. K. (1992), Volatiles In Interplanetary Dust Particles - A Review, *Journal of Geophysical Research-Planets*, *97*(E3), 3865-3875.

Glavin, D. P., et al. (2013), Evidence for Perchlorates and the Origin of Chlorinated Hydrocarbons Detected by SAM at the Rocknest Aeolian Deposit, *Journal of Geophysical Research Planets*, *118*, 1955-1973, doi:10.1002/jgre.20144.

Golden, D. C., D. W. Ming, B. Sutter, B. C. Clark, R. V. Morris, W. V. Boynton, M. H. Hecht, and S. P. Kounaves (2009), Sulfur Mineralogy at the Mars Phoenix Landing Site, in *LPI Contribution No. 1468*, p. 2319, Lunar and Planetary Institute, Houston.

Gooding, J. L. (1978), Chemical Weathering on Mars - Thermodynamic Stabilities of Primary Minerals (and Their Alteration Products) from Mafic Igneous Rocks, *Icarus*, *33*(3), 483-513.

Gooding, J. L. (1992), Soil Mineralogy and Chemistry on Mars - Possible Clues from Salts and Clays in Snc Meteorites, *Icarus*, *99*(1), 28-41.

Gooding, J. L., and D. W. Muenow (1986), Martian Volatiles In Shergottite Eeta 79001 - New Evidence From Oxidized Sulfur And Sulfur-Rich Aluminosilicates, *Geochimica Et Cosmochimica Acta*, *50*(6), 1049-1059, doi:10.1016/0016-7037(86)90387-x.

Grady, M. M., A. B. Verchovsky, and I. P. Wright (2004), Magmatic carbon in Martian meteorites: attempts to constrain the carbon cycle on Mars, *International Journal of Astrobiology*, *3*(2), 117-124.

Greenwood, J. P., L. R. Riciputi, and H. Y. McSween (1997), Sulfide isotopic compositions in shergottites and ALH84001, and possible implications for life on Mars, *Geochimica Et Cosmochimica Acta*, *61*(20), 4449-4453.

Halevy, I., and D. P. Schrag (2009), Sulfur dioxide inhibits calcium carbonate precipitation: Implications for early Mars and Earth, *Geophysical Research Letters*, *36*, doi:10.1029/2009gl040792.

Halevy, I., M. T. Zuber, and D. P. Schrag (2007), A sulfur dioxide climate feedback on early Mars, *Science*, *318*(5858), 1903-1907, doi:10.1126/science.1147039.

Hoare, I. C., and J. H. Levy (1990), The Nonisothermal Reaction-Kinetics Of Pyrite With Water-Vapor, *Thermochimica Acta*, *164*, 153-160, doi:10.1016/0040-6031(90)80432-x.

Hoffman, J. H., R. C. Chaney, and H. Hammack (2008), Phoenix Mars Mission-The Thermal Evolved Gas Analyzer, *Journal of the American Society for Mass Spectrometry*, *19*(10), 1377-1383, doi:10.1016/j.jasms.2008.07.015.

Hong, Y., and B. Fegley (1997a), Formation of carbonyl sulfide (OCS) from carbon monoxide and sulfur vapor and applications to Venus, *Icarus*, *130*(2), 495-504, doi:10.1006/icar.1997.5824.

Hong, Y., and B. Fegley (1997b), The kinetics and mechanism of pyrite thermal decomposition, *Berichte Der Bunsen-Gesellschaft-Physical Chemistry Chemical Physics*, *101*(12), 1870-1881.

Hu, G. L., K. Dam-Johansen, W. Stig, and J. P. Hansen (2006), Decomposition and oxidation of pyrite, *Progress in Energy and Combustion Science*, *32*(3), 295-314, doi:10.1016/j.pecs.2005.11.004.

Hurowitz, J. A., S. M. McLennan, N. J. Tosca, R. E. Arvidson, J. R. Michalski, D. W. Ming, C. Schroder, and S. W. Squyres (2006), In situ and experimental evidence for acidic weathering of rocks and soils on Mars, *Journal of Geophysical Research-Planets*, *111*(E2), E02S19, doi:10.1029/2005JE002515.

Ingraham, T. R., H. W. Parsons, and L. J. Cabri (1972), Leaching Of Pyrrhotite With Hydrochloric-Acid, *Canadian Metallurgical Quarterly*, *11*(2), 407.

Jakosky, B. M., and E. L. Shock (1998), The biological potential of Mars, the early Earth, and Europa, *Journal of Geophysical Research-Planets*, *103*(E8), 19359-19364, doi:10.1029/98je01892.

Jambor, J. L., D. K. Nordstrom, and C. N. Alpers (2000), Metal-sulfate Salts from Sulfide Mineral Oxidation, in *Sulfate Minerals: Crystallography, Geochemistry, and Environmental Significance*, edited by C. N. Alpers, Jambor, J. L., Nordstrom, D. K., pp. 303-350, The Mineralogical Society of America, Washington D.C.

Johnson, S. S., M. A. Mischna, T. L. Grove, and M. T. Zuber (2008), Sulfur-induced greenhouse warming on early Mars, *Journal of Geophysical Research-Planets*, *113*(E8), doi:10.1029/2007je002962.

Jull, A. J. T., J. W. Beck, and G. S. Burr (2000), Isotopic evidence for extraterrestrial organic material in the Martian meteorite, Nakhla, *Geochimica Et Cosmochimica Acta*, *64*(21), 3763-3772, doi:10.1016/s0016-7037(00)00458-0.

Karunatillake, S., O. Gasnault, S. M. McLennan, A. D. Rogers, J. J. Wray, S. W. Squyres, and W. V. Boynton (2012), The Hydration State of Sulfates on Mars, in *LPI Contribution No. 1659,* p. 2940, Lunar and Planetary Institute, Houston.

Karunatillake, S., J. J. Wray, S. W. Squyres, G. J. Taylor, O. Gasnault, S. M. McLennan, W. Boynton, M. R. El Maarry, and J. M. Dohm (2009), Chemically striking regions on Mars and Stealth revisited, *Journal of Geophysical Research-Planets*, *114*, doi:10.1029/2008je003303.

Killops, S., and V. Killops (2005), *Introduction to Organic Geochemistry*, 2nd ed., 393 pp., Blackwell Science Ltd., Malden, MA.

King, P. L., and S. M. McLennan (2010), Sulfur on Mars, *Elements*, *6*(2), 107-112, doi:10.2113/gselements.6.2.107.

King, P. L., and H. Y. McSween (2005), Effects of H_2O, pH, and oxidation state on the stability of Fe minerals on Mars, *Journal of Geophysical Research-Planets*, *110*(E12), doi:10.1029/2005je002482.

Klingelhofer, G., et al. (2004), Jarosite and hematite at Meridiani Planum from Opportunity's Mossbauer spectrometer, *Science*, *306*(5702), 1740-1745.

Kotra, R. K., E. K. Gibson, and M. A. Urbancic (1982), Release of Volatiles from Possible Martian Analogs, *Icarus*, *51*(3), 593-605.

Kounaves, S. P., et al. (2010), Soluble sulfate in the martian soil at the Phoenix landing site, *Geophysical Research Letters*, *37*, L09201, doi:10.1029/2010gl042613.

Kraft, M. D., J. R. Michalski, and T. G. Sharp (2003), Effects of pure silica coatings on thermal emission spectra of basaltic rocks: Considerations for Martian surface mineralogy, *Geophys. Res. Lett.*, *30*(24), 2288, doi:2210.1029/2003GL018848.

Lane, M. D., J. L. Bishop, M. D. Dyar, P. L. King, M. Parente, and B. C. Hyde (2008), Mineralogy of the Paso Robles soils on Mars, *American Mineralogist*, *93*(5-6), 728-739, doi:10.2138/am.2008.2757.

Langevin, Y., F. Poulet, J. P. Bibring, and B. Gondet (2005), Sulfates in the north polar region of Mars detected by OMEGA/Mars express, *Science*, *307*(5715), 1584-1586.

Lauer, H. V. J., P. D. J. Archer, B. Sutter, P. B. Niles, and D. W. Ming (2012), Thermal and Evolved Gas Analysis of Nanophase Carbonates:Implications for Thermal and Evolved Gas Analysis on Mars Missions, in *LPI Contribution No. 1659,* p. 2299, Lunar and Planetary Institute, Houston.

Leshin, L. A., et al. (2013), Volatile, Isotope, and Organic Analysis of Martian Fines with the Mars Curiosity Rover, *Science*, *341*(6153), doi:10.1126/science.1238937.

Lindsay, W. L. (1979), *Chemical Equilibria in Soils*, 449 pp., Blackburn Press, Caldwell, NJ.

Lorand, J. P., V. Chevrier, and V. Sautter (2005), Sulfide mineralogy and redox conditions in some shergottites, *Meteoritics & Planetary Science*, *40*(8), 1257-1272.

Luo, D. L., C. X. Zhang, P. L. Leung, Z. L. Deng, and M. J. Stokes (1998), Investigation of ESR, TL and positron annihilation in gamma-ray irradiated magnesium sulphate, *Journal of Physics D-Applied Physics*, *31*(7), 906-912.

Mahaffy, P. R., et al. (2012), The Sample Analysis at Mars Investigation and Instrument Suite, *Space Science Reviews*, *170*(1-4), 401-478, doi:10.1007/s11214-012-9879-z.

Mangold, N., L. Roach, R. Milliken, S. Le Mouelic, V. Ansan, J. P. Bibring, P. Masson, J. F. Mustard, S. Murchie, and G. Neukum (2010), A Late Amazonian alteration layer related to local volcanism on Mars, *Icarus*, *207*(1), 265-276, doi:10.1016/j.icarus.2009.10.015.

Marion, G. M., J. S. Kargel, J. K. Crowley, and D. C. Catling (2013), Sulfite–sulfide–sulfate–carbonate equilibria with applications to Mars, *Icarus*, *225*, 342-351.

McCoy, T. J., G. J. Taylor, and K. Keil (1992), Zagami - Product Of A 2-Stage Magmatic History, *Geochimica Et Cosmochimica Acta*, *56*(9), 3571-3582, doi:10.1016/0016-7037(92)90400-d.

McCubbin, F. M., N. J. Tosca, A. Smirnov, H. Nekvasil, A. Steele, M. Fries, and D. H. Lindsley (2009), Hydrothermal jarosite and hematite in a pyroxene-hosted melt inclusion in martian meteorite Miller Range (MIL) 03346: Implications for magmatic-hydrothermal fluids on Mars, *Geochimica Et Cosmochimica Acta*, *73*(16), 4907-4917, doi:10.1016/j.gca.2009.05.031.

McLennan, S. M. (2012), Geochemistry of sedimentary processes on Mars. , in *Mars Sedimentology*, edited by J. P. Grotzinger and R. E. Milliken, pp. 119-138, SEPM Spec. Publ.

McLennan, S. M., W. V. Boynton, S. Karunatillake, B. C. Hahn, G. J. Taylor, and M. O. G. Team (2010), Distribution of Sulfur on the Surface of Mars Determined by the 2001 Mars Odyssey Gamma Ray Spectrometer, in *LPI Contribution No. 1533*, p. 2174, Lunar and Planetary Institute, Houston.

McLennan, S. M., and J. P. Grotzinger (2008), The sedimentary rock cycle of Mars, in *The Martian Surface: Composition, Mineralogy, and Physical Properties*, edited by J. F. Bell, pp. 541-577, Cambridge Univ. Press, Cambridge.

McSween, H. Y., and K. Keil (2000), Mixing relationships in the Martian regolith and the composition of globally homogeneous dust, *Geochimica Et Cosmochimica Acta*, *64*(12), 2155-2166.

Michalski, J. R., M. D. Kraft, T. G. Sharp, L. B. Williams, and P. R. Christensen (2006), Emission spectroscopy of clay minerals and evidence for poorly crystalline aluminosilicates on Mars from Thermal Emission Spectrometer data, *Journal of Geophysical Research-Planets*, *111*(E3), doi: 10.1029/2005JE002438.

Milliken, R. E., J. P. Grotzinger, and B. J. Thomson (2010), Paleoclimate of Mars as captured by the stratigraphic record in Gale Crater, *Geophysical Research Letters*, *37*, L04201, doi:10.1029/2009gl041870.

Milliken, R. E., et al. (2008), Opaline silica in young deposits on Mars, *Geology*, *36*(11), 847-850, doi:10.1130/g24967a.1.

Milodowski, A. E., and D. J. Morgan (1980), Identification and Estimation of Carbonate Minerals at Low-Levels by Evolved Co2 Analysis, *Nature*, *286*(5770), 248-249.

Ming, D. W., et al. (2006), Geochemical and mineralogical indicators for aqueous processes in the Columbia Hills of Gusev crater, Mars, *Journal of Geophysical Research-Planets*, *111*(E2), E02s12, doi:10.1029/2005je002560.

Morgan, D. J., S. B. Warrington, and S. S. J. Warne (1988), Earth Sciences Applications of Evolved Gas-Analysis - a Review, *Thermochimica Acta*, *135*, 207-212.

Morris, R. V., et al. (2000), Mineralogy, composition, and alteration of Mars Pathfinder rocks and soils: Evidence from multispectral, elemental, and magnetic data on terrestrial analogue, SNC meteorite, and Pathfinder samples, *Journal of Geophysical Research-Planets*, *105*(E1), 1757-1817.

Morris, R. V., et al. (2008), Iron mineralogy and aqueous alteration from Husband Hill through Home Plate at Gusev Crater, Mars: Results from the Mossbauer instrument on the Spirit Mars Exploration Rover, *Journal of Geophysical Research-Planets*, *113*(E12), E12s42, doi:10.1029/2008je003201.

Morris, R. V., et al. (2006), Mossbauer mineralogy of rock, soil, and dust at Meridiani Planum, Mars: Opportunity's journey across sulfate-rich outcrop, basaltic sand and dust, and hematite lag deposits, *Journal of Geophysical Research-Planets*, *111*(E12), doi:10.1029/2006je002791.

Morris, R. V., et al. (2013), The Amorphous Component in Martian Basaltic Soil in Global Perspective from MSL and MER Missions, in *LPI Contribution No. 1719,* p. 1653, Lunar and Planetary Institute, Houston.

Newsom, H. E., J. J. Hagerty, and F. Goff (1999), Mixed hydrothermal fluids and the origin of the Martian soil, *Journal of Geophysical Research-Planets*, *104*(E4), 8717-8728.

Niles, P. B., and J. Michalski (2009), Meridiani Planum sediments on Mars formed through weathering in massive ice deposits, *Nature Geoscience*, *2*(3), 215-220, doi:10.1038/ngeo438.

Parfitt, R. L., and R. S. C. Smart (1978), Mechanism of Sulfate Adsorption on Iron-Oxides, *Soil Science Society of America Journal*, *42*(1), 48-50.

Rampe, E. B., and R. V. Morris (in prep), Recognizing sulfate- and phosphate-adsorbed onto nanophase weathering products on Mars using in-situ and remote observations.

Rieder, R., T. Economou, H. Wanke, A. Turkevich, J. Crisp, J. Bruckner, G. Dreibus, and H. Y. McSween (1997), The chemical composition of Martian soil and rocks

returned by the mobile alpha proton x-ray spectrometer: Preliminary results from the x-ray mode, *Science*, *278*(5344), 1771-1774.

Sephton, M. A. (2012), Pyrolysis and mass spectrometry studies of meteoritic organic matter, *Mass Spectrometry Reviews*, *31*(5), 560-569, doi:10.1002/mas.20354.

Sephton, M. A., I. P. Wright, I. Gilmour, J. W. de Leeuw, M. M. Grady, and C. T. Pillinger (2002), High molecular weight organic matter in martian meteorites, *Planetary and Space Science*, *50*(7-8), 711-716, doi:10.1016/s0032-0633(02)00053-3.

Settle, M. (1979), Formation And Deposition Of Volcanic Sulfate Aerosols On Mars *Journal of Geophysical Research*, *84*, 8343-8354, doi:10.1029/JB084iB14p08343.

Shao, D. K., E. J. Hutchinson, J. Heidbrink, W. P. Pan, and C. L. Chou (1994), Behavior of Sulfur During Coal Pyrolysis, *Journal of Analytical and Applied Pyrolysis*, *30*(1), 91-100, doi:10.1016/0165-2370(94)00807-8.

Squyres, S. W., et al. (2012), Ancient Impact and Aqueous Processes at Endeavour Crater, Mars, *Science*, *336*(6081), 570-576, doi:10.1126/science.1220476.

Squyres, S. W., and A. H. Knoll (2005), Sedimentary rocks at Meridiani Planum: Origin, diagenesis, and implications for life on Mars, *Earth and Planetary Science Letters*, *240*(1), 1-10.

Steele, A., et al. (2013), Organic Carbon Inventory of the Tissint Meteorite, in *LPI Contribution No. 1719,* p.2854, Lunar and Planetary Institute, Houston.

Steele, A., et al. (2012), A Reduced Organic Carbon Component in Martian Basalts, *Science*, *337*(6091), 212-215, doi:10.1126/science.1220715.

Steininger, H., F. Goesmann, and W. Goetz (2012), Influence of magnesium perchlorate on the pyrolysis of organic compounds in Mars analogue soils, *Planetary and Space Science*, *71*(1), 9-17, doi:10.1016/j.pss.2012.06.015.

Summons, R. E., J. P. Amend, D. Bish, R. Buick, G. D. Cody, D. J. Des Marais, G. Dromart, J. L. Eigenbrode, A. H. Knoll, and D. Y. Sumner (2011), Preservation of Martian Organic and Environmental Records: Final Report of the Mars Biosignature Working Group, *Astrobiology*, *11*(2), 157-181, doi:10.1089/ast.2010.0506.

Sutter, B., W. V. Boynton, D. W. Ming, A. B. Niles, R. V. Morris, D. C. Golden, H. V. Lauer, C. Fellows, D. K. Hamara, and S. A. Mertzman (2012), The detection of carbonate in the martian soil at the Phoenix Landing site: A laboratory investigation and comparison with the Thermal and Evolved Gas Analyzer (TEGA) data, *Icarus*, *218*(1), 290-296, doi:10.1016/j.icarus.2011.12.002.

Tani, A., N. Hasegawa, K. Norizawa, T. Yada, and M. Ikeya (2012), Radiation-induced radicals in hydrated magnesium sulfate, *Radiation Measurements*, *47*(9), 890-893, doi:10.1016/j.radmeas.2012.03.006.

Tosca, N. J., S. M. McLennan, M. D. Dyar, E. C. Sklute, and F. M. Michel (2008), Fe oxidation processes at Meridiani Planum and implications for secondary Fe mineralogy on Mars, *Journal of Geophysical Research-Planets*, *113*(E5), doi:10.1029/2007je003019.

Tosca, N. J., S. M. McLennan, D. H. Lindsley, and M. A. A. Schoonen (2004), Acid-sulfate weathering of synthetic Martian basalt: The acid fog model revisited, *Journal of Geophysical Research-Planets*, *109*(E05003), doi:10.1029/2003JE002218.

Uno, T. (1951), Equilbrium between FeS and mixed gas of H2 and H2O, *Memoirs of the Faculty of Engineering, Hokkaido University*, *9*(1), 84-90, doi:http://hdl.handle.net/2115/37768.

Vaniman, D. T., D. L. Bish, S. J. Chipera, C. I. Fialips, J. W. Carey, and W. C. Feldman (2004), Magnesium sulphate salts and the history of water on Mars, *Nature*, *431*(7009), 663-665, doi:10.1038/nature02973.

Vinodkumar, M., C. Limbachiya, and H. Bhutadia (2010), Electron impact calculations of total ionization cross sections for environmentally sensitive diatomic and triatomic molecules from threshold to 5 keV, *Journal of Physics B-Atomic Molecular and Optical Physics*, *43*(1), doi:10.1088/0953-4075/43/1/015203.

Wang, A., et al. (2006), Sulfate deposition in subsurface regolith in Gusev crater, Mars, *Journal of Geophysical Research-Planets*, *111*(E2), E02s17, doi:10.1029/2005je002513.

Wang, A., and Z. C. Ling (2011), Ferric sulfates on Mars: A combined mission data analysis of salty soils at Gusev crater and laboratory experimental investigations, *Journal of Geophysical Research-Planets*, *116*, doi:10.1029/2010je003665.

Wiseman, S. M., R. E. Arvidson, R. V. Morris, F. Poulet, J. C. Andrews-Hanna, J. L. Bishop, S. L. Murchie, F. P. Seelos, D. Des Marais, and J. L. Griffes (2010), Spectral and stratigraphic mapping of hydrated sulfate and phyllosilicate-bearing deposits in northern Sinus Meridiani, Mars, *Journal of Geophysical Research-Planets*, *115*, doi:10.1029/2009je003354.

Wray, J. J., et al. (2011), Columbus crater and other possible groundwater-fed paleolakes of Terra Sirenum, Mars, *Journal of Geophysical Research-Planets*, *116*, doi:10.1029/2010je003694.

Wray, J. J., S. L. Murchie, S. W. Squyres, F. P. Seelos, and L. L. Tornabene (2009), Diverse aqueous environments on ancient Mars revealed in the southern highlands, *Geology*, *37*(11), 1043-1046, doi:10.1130/g30331a.1.

Wray, J. J., S. W. Squyres, L. H. Roach, J. L. Bishop, J. F. Mustard, and E. Z. N. Dobrea (2010), Identification of the Ca-sulfate bassanite in Mawrth Vallis, Mars, *Icarus*, *209*(2), 416-421, doi:10.1016/j.icarus.2010.06.001.

Xu, L., J. L. Yang, Y. M. Li, and Z. Y. Liu (2004), Behavior of organic sulfur model compounds in pyrolysis under coal-like environment, *Fuel Processing Technology*, *85*(8-10), 1013-1024, doi:10.1016/j.fuproc.2003.11.036.

Yen, A. S., et al. (2013), Evidence for a Global Martian Soil Composition Extends to Gale Crater, in *LPI Contribution No. 1719,* p. 2495, Lunar and Planetary Institute, Houston.

Yen, A. S., et al. (2005), An integrated view of the chemistry and mineralogy of martian soils, *Nature*, *436*(7047), 49-54, doi:10.1038/nature03637.

Yen, A. S., et al. (2008), Hydrothermal processes at Gusev Crater: An evaluation of Paso Robles class soils, *Journal of Geophysical Research-Planets*, *113*(E6), E06s10, doi:10.1029/2007je002978.

Zega, T. J., C. M. O. Alexander, H. Busemann, L. R. Nittler, P. Hoppe, R. M. Stroud, and A. F. Young (2010), Mineral associations and character of isotopically anomalous organic material in the Tagish Lake carbonaceous chondrite, *Geochimica Et Cosmochimica Acta*, *74*(20), 5966-5983, doi:10.1016/j.gca.2010.07.018.

Zhang, T. W., G. S. Ellis, Q. S. Ma, A. Amrani, and Y. C. Tang (2012), Kinetics of uncatalyzed thermochemical sulfate reduction by sulfur-free paraffin, *Geochimica Et Cosmochimica Acta*, *96*, 1-17, doi:10.1016/j.gca.2012.08.010.

Zhang, T. W., G. S. Ellis, C. C. Walters, S. R. Kelemen, K. S. Wang, and Y. C. Tang (2008), Geochemical signatures of thermochemical sulfate reduction in controlled hydrous pyrolysis experiments, *Organic Geochemistry*, *39*(3), 308-328, doi:10.1016/j.orggeochem.2007.12.007.

Zhang, T. W., G. S. Ellis, K. S. Wang, C. C. Walters, S. R. Kelemen, B. Gillaizeau, and Y. C. Tang (2007), Effect of hydrocarbon type on thermochemical sulfate

reduction, *Organic Geochemistry*, *38*(6), 897-910, doi:10.1016/j.orggeochem.2007.02.004.

Zolotov, M. Y., and E. L. Shock (2005), Formation of jarosite-bearing deposits through aqueous oxidation of pyrite at Meridiani Planum, Mars, *Geophysical Research Letters*, *32*(21), doi:10.1029/2005gl024253.

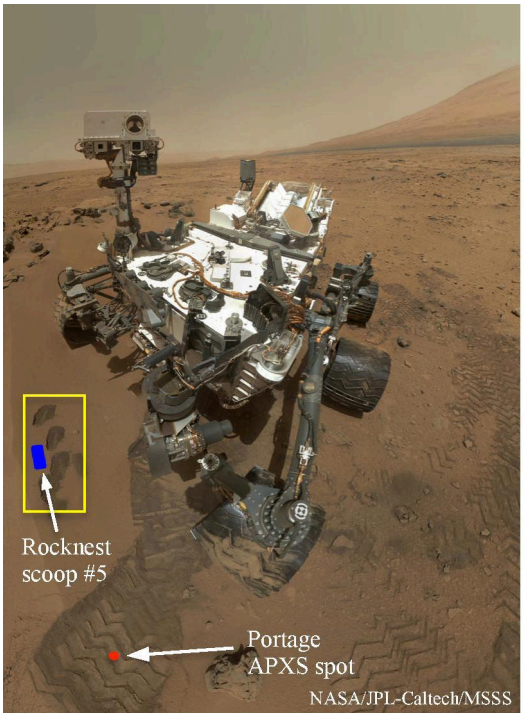

Figure 1. Mars Hand Lens Imager (MAHLI) self-portrait of the Mars Science Laboratory (MSL) rover *Curiosity* at the Rocknest sand shadow. The yellow box highlights the area of sample scoops, and the blue box shows the approximate location of Rocknest scoop #5. After scoop #5 material was sieved to <150 μm, subsamples were delivered to the SAM and CheMin instruments. Rover wheel width is 40 cm.

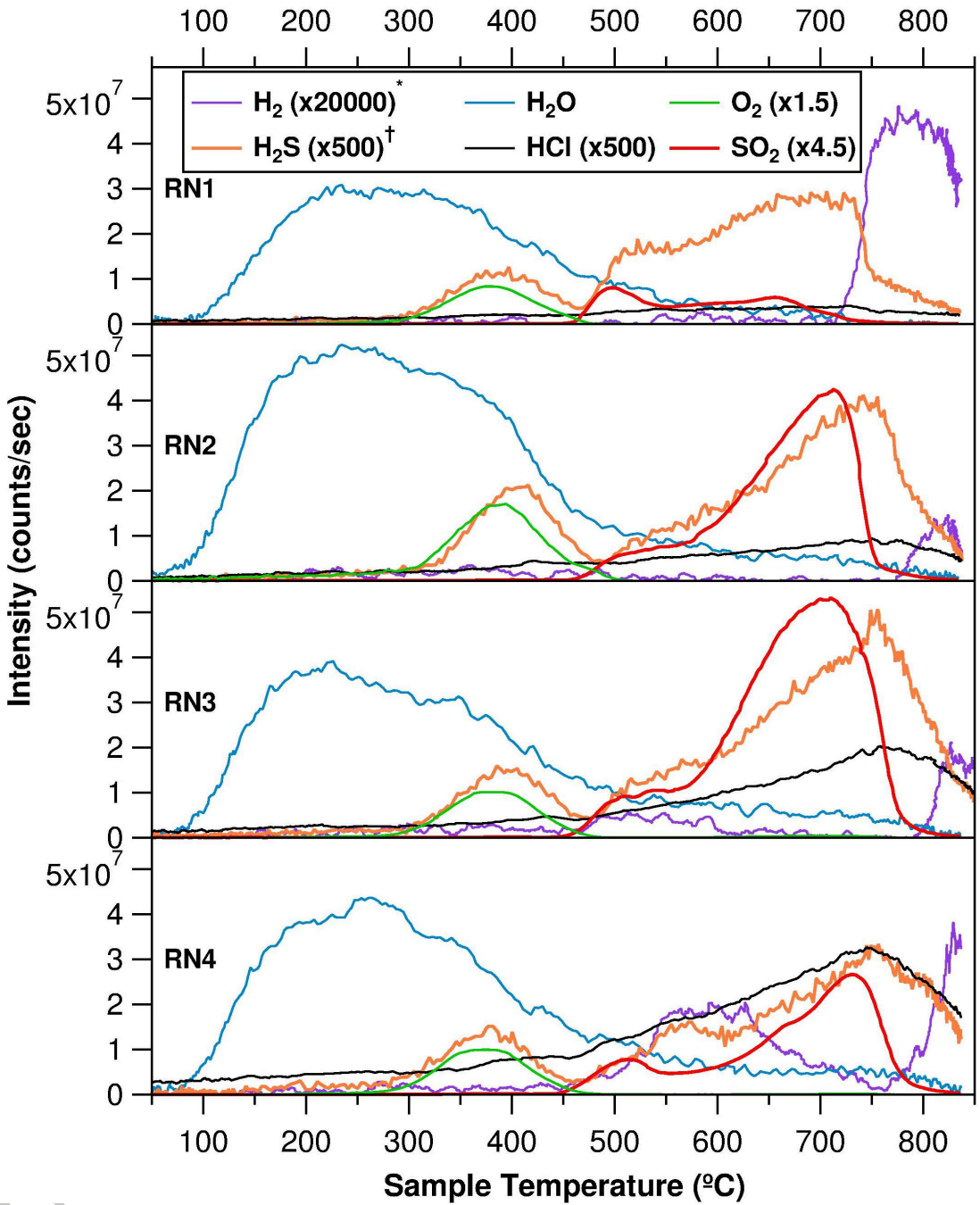

Figure 2. SO_2 and H_2S traces from each Rocknest scoop #5 subsample run (RN1-RN4), together with the EGA traces of several other Rocknest volatiles that may play a part in the evolution of SO_2 and H_2S (see section 4). * In SAM Rocknest analyses, mass-to-charge ratio (m/z) 2, which is the main mass for H_2 (2 Da), was not monitored. The m/z 3, however, was monitored. This mass can be attributed to isotopologues and MS source ionization products of H_2 (HD and H^{3+}, respectively), as well as some possible contributions from ^{3}He. †m/z 34 can be attributed to H_2S, but can also include some contributions from the ^{34}S fragment of SO_2 and an isotopologue of O_2 (see section 3.2). (*The vast majority of the peak in m/z 34 (H_2S) EGA trace intensity near 400 °C is coincident with the large O_2 peak evolved from Rocknest and results from the O_2 isotopologue ($^{16}O^{18}O$), not H_2S)).*

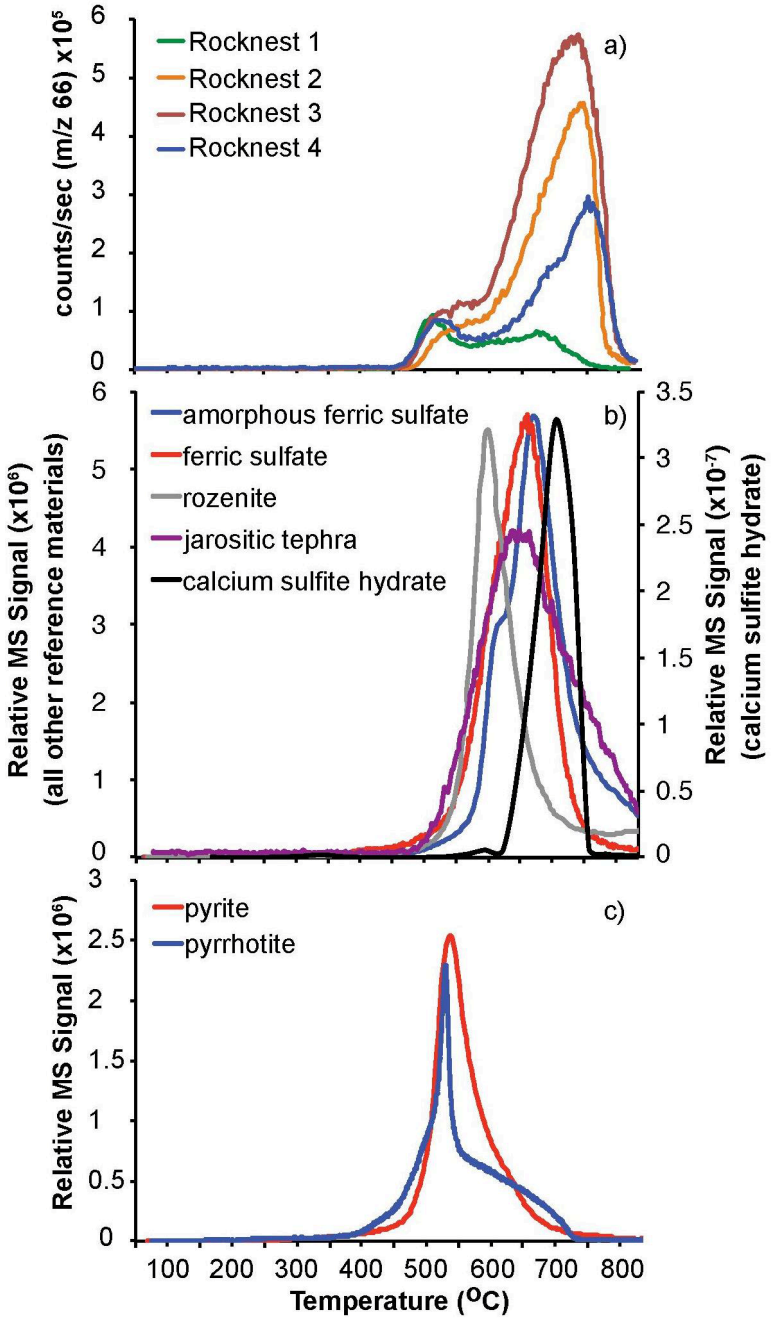

Figure 3. a) SO_2 (m/z 66) SAM EGA-MS traces from each Rocknest sample. b) and c) SAM-like EGA-MS SO_2 (m/z 64) traces from several sulfur-bearing phase reference materials, for comparison with Rocknest data.

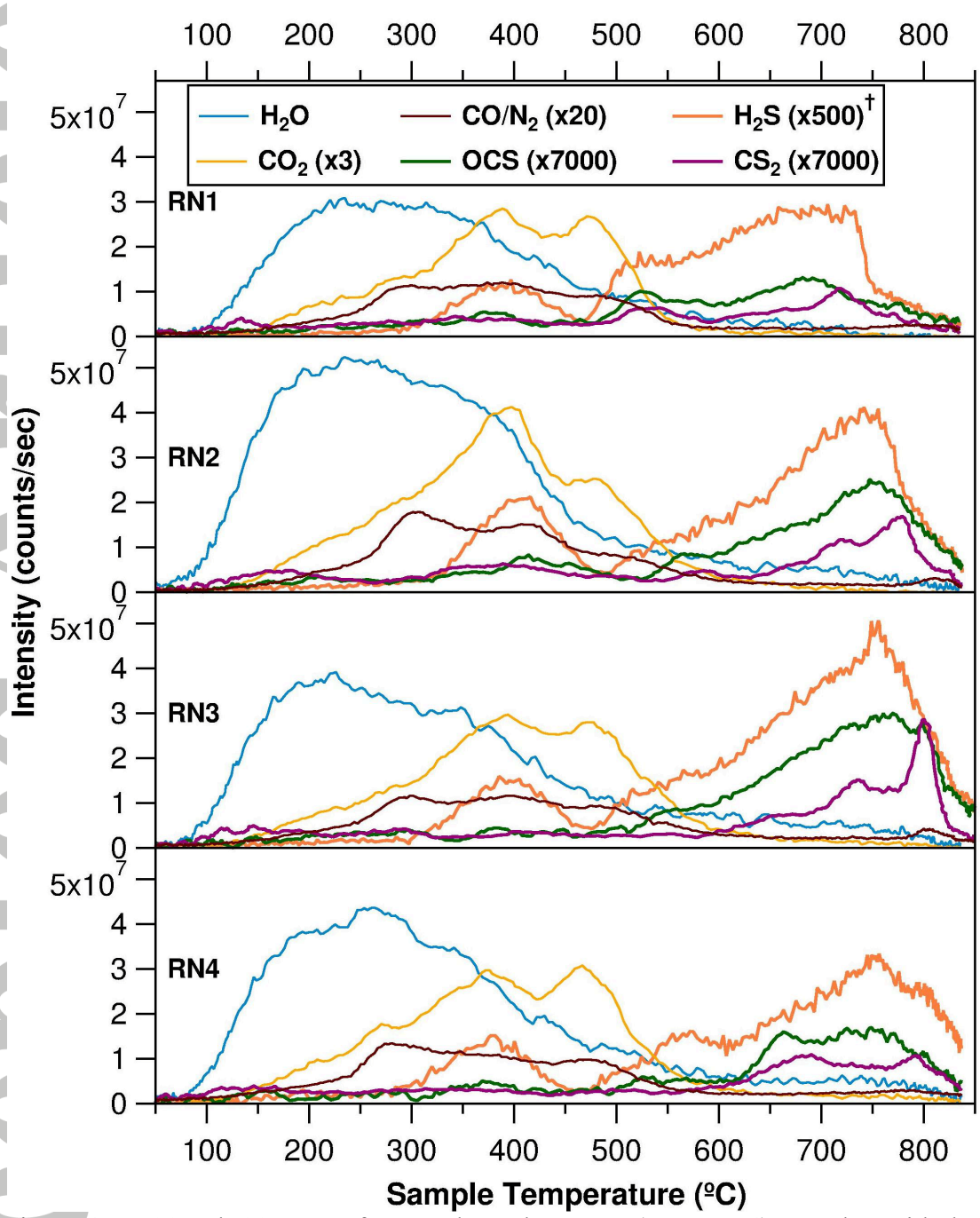

Figure 4. OCS and CS_2 traces from each Rocknest run (RN1-RN4), together with the EGA traces of several other Rocknest volatiles that may play a part in the detection of OCS and CS_2 evolved from Rocknest subsamples (see section 4). †m/z 34 can be attributed to H_2S, but can also include some contributions from the ^{34}S fragment of SO_2 and an isotopologue of O_2 (see section 3.2). (*The vast majority of the peak in m/z 34 (H_2S) EGA trace intensity in this figure near 400 ^{o}C is coincident with the large O_2 peak evolved from Rocknest materials (see Figure 2 for O_2 trace) and results from the O_2 isotopologue ($^{16}O^{18}O$), not H_2S)).*

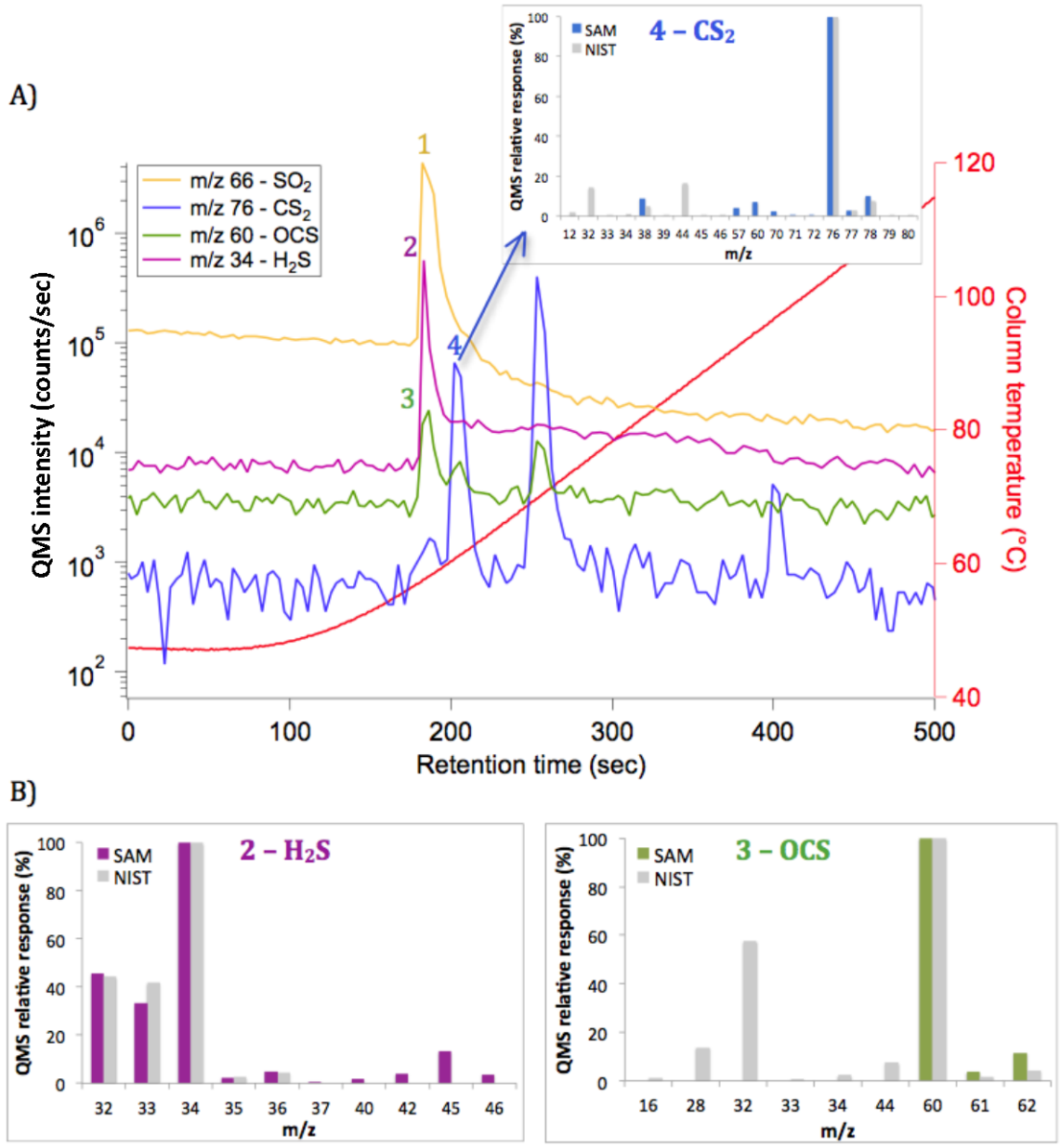

Figure 5. a) GCMS analysis of Rocknest volatiles H_2S, OCS and CS_2 displayed as traces of m/z 34, 60 and 76 respectively. The column used is SAM GC5, holding a CLP-like capillary phase. The temperature of the column is plotted as a red line. m/z 66, 60 and 76 are plotted from Rocknest 3. m/z 34 is plotted from Rocknest 2, with a corrected retention time. m/z 66 (yellow line) is chosen for tracking the detection of SO_2, as the base peak of SO_2 (m/z 64) leads to a saturation of the detector. SO_2 is displayed as a reference for retention time. The peaks are labeled 1 to 4 and represent the S-bearing compounds. The inset shows the mass spectrum for peak 4 compared to that for CS_2 from NIST (National Institute for Standards and Technology). b) Mass spectra for H_2S and OCS identified by comparison to the NIST11 reference library.

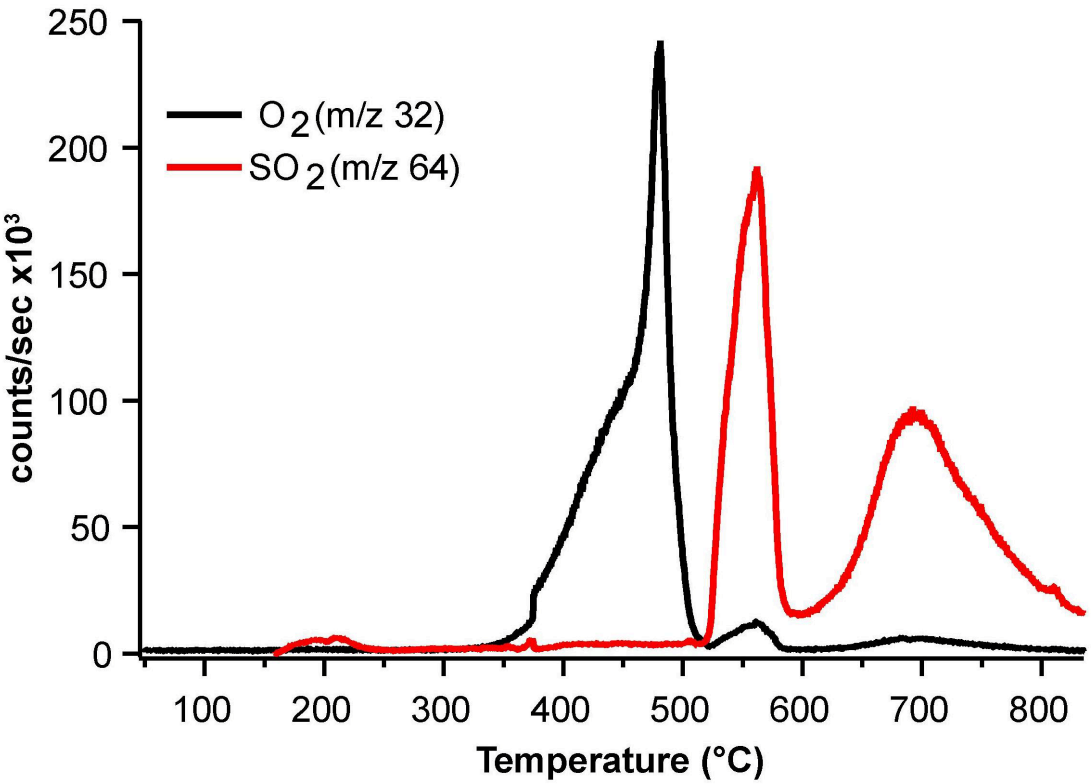

Figure 6. SO_2 (m/z 64) and O_2 (m/z 32) traces from a SAM-like laboratory EGA analysis of a 1:1 Ca-perchlorate/pyrite mixture in an inert matrix (fused silica powder).

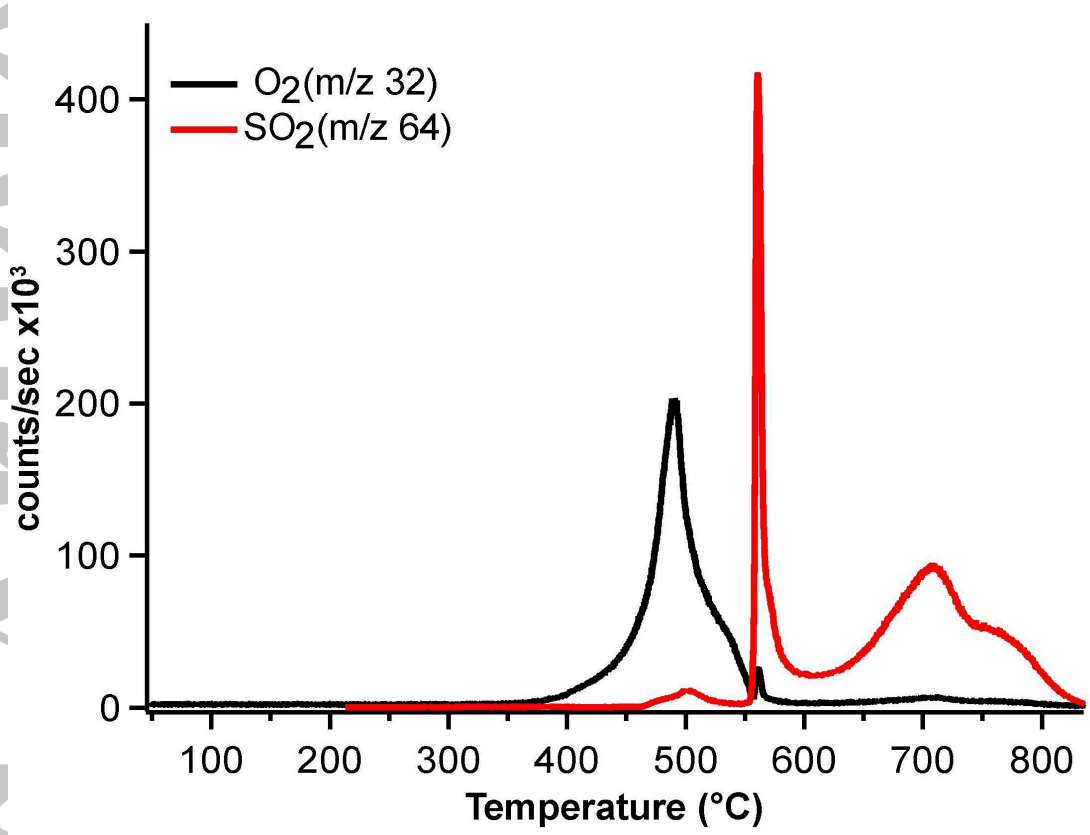

Figure 7. SO_2 (m/z 64) and O_2 (m/z 32) traces from a SAM-like laboratory EGA analysis of a 1:1 Ca-perchlorate/pyrrhotite mixture in an inert matrix (fused silica powder).

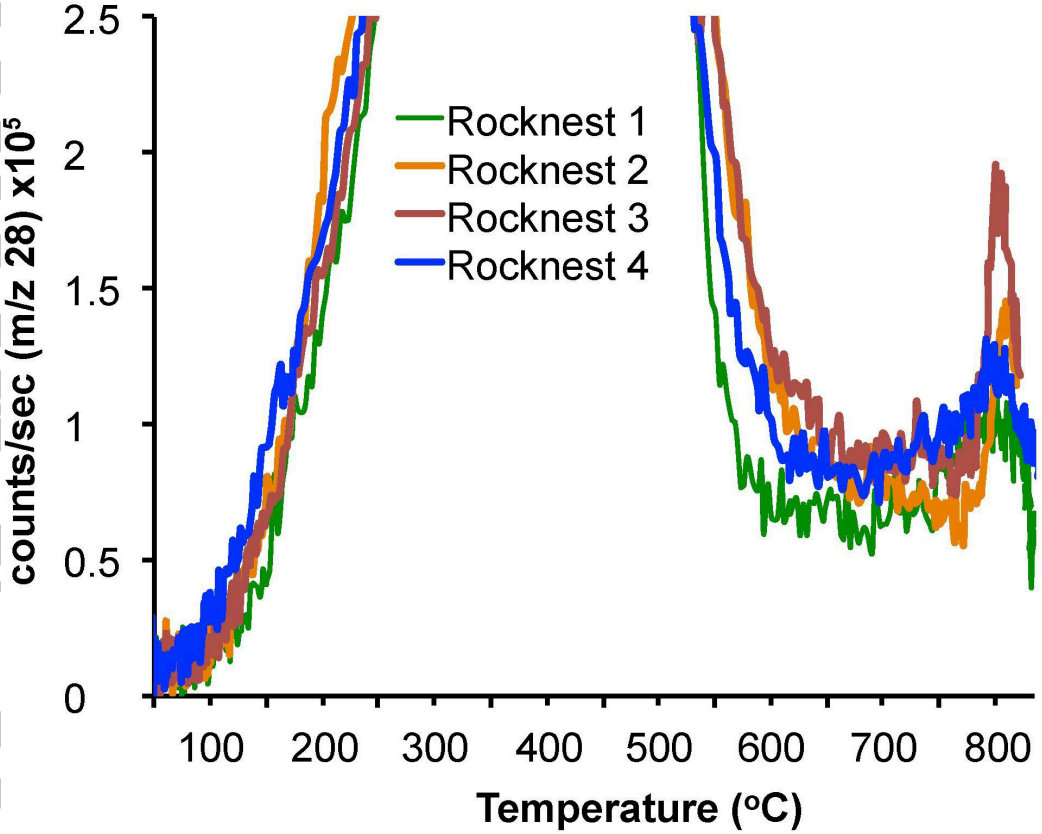

Figure 8. m/z 28 (can be attributed to CO and/or N_2) EGA traces from Rocknest runs, scaled to show the presence of small amounts of possible CO detected at high temperatures.

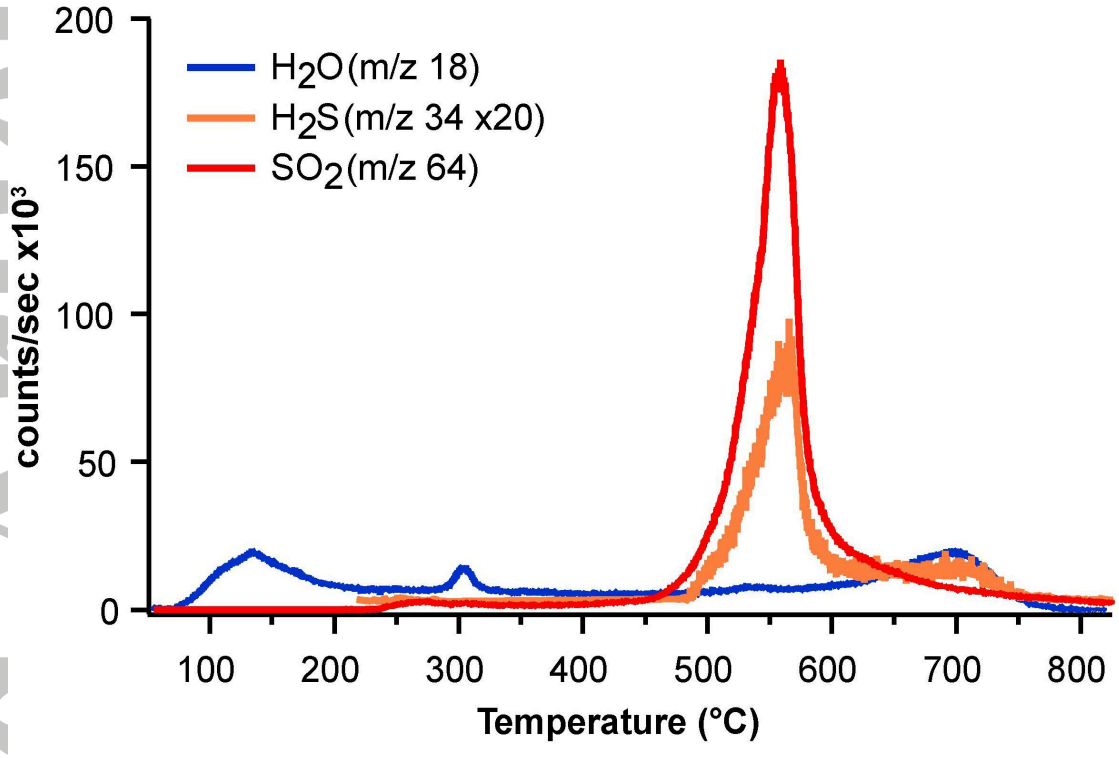

Figure 9. SO_2, H_2O and H_2S traces from a SAM-like laboratory EGA analysis of a pyrite/montmorillonite mixture in an inert matrix (fused silica powder).

Table 1. Analog materials, analysis system used, and source.

Sample	Formula	Analysis System*	Source
Pyrite	FeS_2	S	Natural, PYCSD1 (Custer, SD; R. Morris collection)
Pyrrhotite	$Fe_{(1-x)}S$	A	Natural, SAEUMX01 (Santa Eulaia, MX; R. Morris collection)
Ferric sulfate hydrate	$Fe^{3+}SO_4•H_2O$	A	Synthetic (Sigma-Aldrich)
Rozenite	$Fe^{2+}SO_4•4H_2O$	S	Synthetic (Sigma-Aldrich)
Kieserite	$MgSO_4•H_2O$	H	Synthetic (ESTA)
Epsomite	$MgSO_4•7H_2O$	H	Synthetic (Sigma-Aldrich)
Calcium sulfite hydrate	$CaSO_3•H_2O$	H	Synthetic (Sigma-Aldrich)
Amorphous ferric sulfate	$(Fe_2O_3)(SO_3)_3(H_2O)_{5.4}$ (empirical composition)	S	Synthetic, DC504LN-D01; (Cryoprecipitation; [*Morris et al.*, in prep.])
Jarositic tephra	$KFe_3(SO_4)_2(OH)_6$ (jarosite)	S	Natural tephra, HWMK979 (Mauna Kea, HI; same as HWMK620 [*Morris et al.*, 2000])
Calcium perchlorate tetrahydrate/ pyrite mixture	$Ca(ClO_4)_2•4H_2O/FeS_2$, 1:1 mixture	A	Synthetic (Sigma-Aldrich)/ Natural, PYCSD1 (Custer, SD; R. Morris collection)
Calcium perchlorate tetrahydrate/ pyrrhotite mixture	$Ca(ClO_4)_2•4H_2O$/ $Fe_{(1-x)}S$, 1:1 mixture	A	Synthetic (Sigma-Aldrich)/ Natural, SAEUMX01 (Santa Eulaia, MX; R. Morris collection)
Montmorillonite	$(Na,Ca)_{0.3}(Al,Mg)_2 Si_4O_{10}(OH)_2•nH_2O$	A	Natural, SWy-2 (Clay Mineral Society)

*S, SAM breadboard; H, Hiden EGA-MS system; A, Agilent EGA-MS system.

Table 2. Abundances of SO_2 and H_2S, OCS, and CS_2 evolved from Rocknest fines over the SAM pyrolysis temperature range.

	Downlink Sol	SO_2 molar abundance (µmole) [a 1]	SO_3 equivalent Sample Weight % [b 1]	H_2S abundance (nanomole)[c]	OCS abundance (nanomole)[c]	CS_2 abundance (nanomole)[c]
Rocknest 1	094	3.1 ± 0.2	0.5 ± 0.1	41 ± 8	1.2 ± 0.24	0.20 ± 0.04
Rocknest 2	097	14.7 ± 2.0	2.4 ± 0.5	81 ± 16	3.5 ± 0.7	0.87 ± 0.17
Rocknest 3	101	23.3 ± 3.1	3.7 ± 0.8	109 ± 21	4.8 ± 1.0	1.0 ± 0.20
Rocknest 4	118	11.2 ± 1.4	1.8 ± 0.4	77 ± 15	2.6 ± 0.52	0.71 ± 0.14

[1] *Leshin et al.*, 2013.
[a]Errors (i.e., precision) reported for molar abundances are the 2σ standard deviation from the mean of calculations done using different m/z values for the same species.
[b]Weight % values were calculated using an estimated sample mass of 50 ± 8 mg (2σ), with errors propagated including the uncertainty in molar abundance.
[c]Errors for trace species are estimated conservatively at 20% due to sources including statistical noise, variations in calibration runs, background subtraction, interferences from other compounds, and assumptions about instrument effects such as ionization efficiencies and fragmentation patterns.